INTERNALIZATION AND TOXICITY OF POLYSTYRENE NANOPLASTICS ON INMORTALIZED HUMAN NEURAL STEM CELLS

Mª Carmen González-Caballero[a*], Mercedes de Alba González[a], Mónica Torres-Ruiz[a], Patricia Iglesias-Hernández[a,c], Verónica Zapata[c], María C. Terrón[d], Martin Sachse[d], Mónica Morales[b], Raquel Martin-Folgar[b], Isabel Liste [c], Ana I. Cañas-Portilla[a]

[a]Área de Toxicología Ambiental, Centro Nacional de Sanidad Ambiental (CNSA), Instituto de Salud Carlos III (ISCIII), Ctra. Majadahonda-Pozuelo Km. 2,2., 28220, Majadahonda (Madrid), Spain

[b]Grupo de Biología y Toxicología Ambiental, Departamento de Física Matemática y de Fluidos, Facultad de Ciencias, UNED. Urbanización Monte Rozas, Avda. Esparta s/n, Ctra. de Las Rozas al Escorial Km 5, 28232, Las Rozas (Madrid), Spain.

[c]Unidad Funcional de Enfermedades Crónicas, Instituto de Salud Carlos III (ISCIII), Ctra. Majadahonda-Pozuelo Km. 2,2., 28220, Majadahonda (Madrid), Spain.

[d]Unidad de Microscopía Electrónica, Unidades Centrales Científico Técnicas, Instituto de Salud Carlos III (ISCIII), Ctra. Majadahonda-Pozuelo Km. 2,2., 28220, Majadahonda (Madrid), Spain.

* Corresponding author

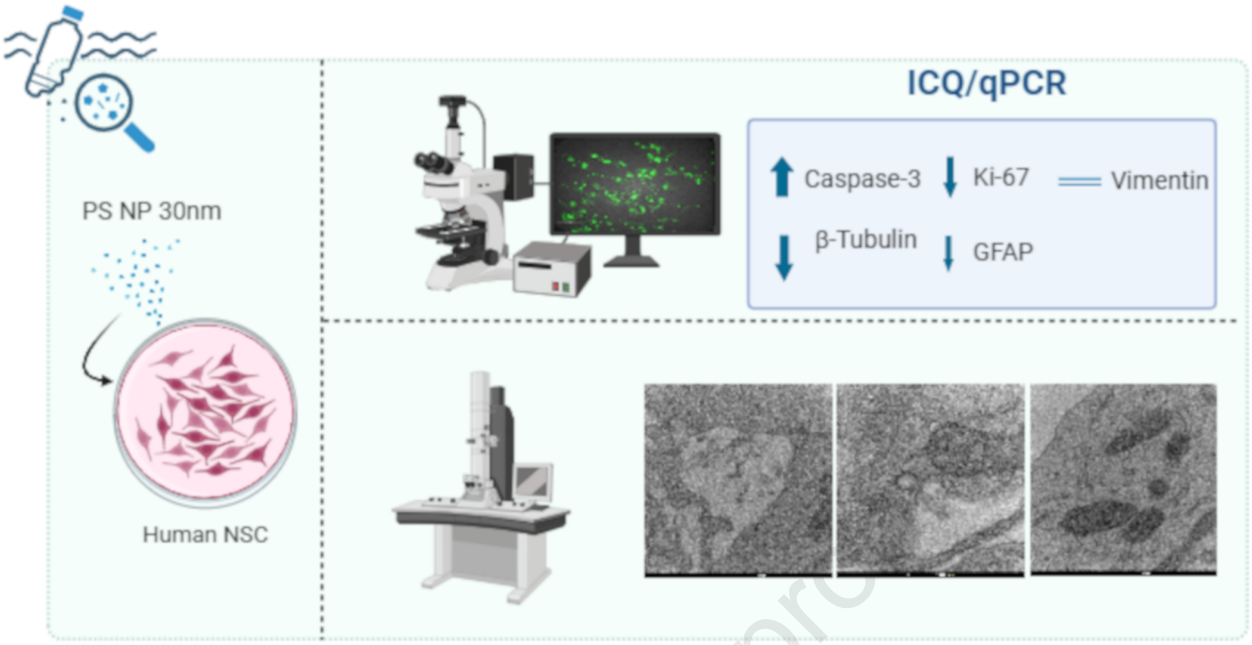

INTERNALIZATION AND TOXICITY OF POLYSTYRENE NANOPLASTICS ON INMORTALIZED HUMAN NEURAL STEM CELLS

Mª Carmen González-Caballero[a*], Mercedes de Alba González[a], Mónica Torres-Ruiz[a], Patricia Iglesias-Hernández[a,c], Verónica Zapata[c], María C. Terrón[d], Martin Sachse[d], Mónica Morales[b], Raquel Martin-Folgar[b], Isabel Liste [c], Ana I. Cañas-Portilla[a]

[a]Área de Toxicología Ambiental, Centro Nacional de Sanidad Ambiental (CNSA), Instituto de Salud Carlos III (ISCIII), Ctra. Majadahonda-Pozuelo Km. 2,2., 28220, Majadahonda (Madrid), Spain

[b]Grupo de Biología y Toxicología Ambiental, Departamento de Física Matemática y de Fluidos, Facultad de Ciencias, UNED. Urbanización Monte Rozas, Avda. Esparta s/n, Ctra. de Las Rozas al Escorial Km 5, 28232, Las Rozas (Madrid), Spain.

[c]Unidad Funcional de Enfermedades Crónicas, Instituto de Salud Carlos III (ISCIII), Ctra. Majadahonda-Pozuelo Km. 2,2., 28220, Majadahonda (Madrid), Spain.

[d]Unidad de Microscopía Electrónica, Unidades Centrales Científico Técnicas, Instituto de Salud Carlos III (ISCIII), Ctra. Majadahonda-Pozuelo Km. 2,2., 28220, Majadahonda (Madrid), Spain.

* Corresponding author

ABSTRACT

Global plastic production has increased exponentially in recent decades, and a significant part of it persists in the environment, where it degrades into microplastics and nanoplastics (MPs and NPs). These can enter in humans by ingestion, inhalation, and dermal routes, and there is scientific evidence that they are able to reach the systemic circulation and penetrate and accumulate in various tissues and organs. Neurodevelopmental toxicity of NPs is one of the most worrying effects, as they can cross the blood-brain barrier. In the following study, we analyzed, by transmission electron microscopy, the *in vitro* uptake of 30-nm polystyrene nanoplastics (PS-NPs) into human neural stem cells (NSCs), their accumulation and subcellular localization within the cell. Furthermore, we studied the effects of different concentrations of PS-NPs on cell death, proliferation, and cell differentiation using immunocytochemistry and quantitative real time PCR for specific markers. This study demonstrated that PS-NPs were able to enter the cell, probably by endocytosis, accumulate, and

aggregated in human NSCs, without being detected in the nucleus, causing cell death by apoptosis and decreased cell proliferation. This study provides new insights into the interaction and effects of PS-NPs in human NSC and supports the scientific evidence for the involvement of nanoplastic in neurodevelopmental disorders.

KEYWORDS: human Neural Stem Cells, nanoplastics, uptake, cell death, cell proliferation.

1. INTRODUCTION

The exponential increase in the production, consumption, and global disposal of plastic products since the mid-20th century ("Plastics Europe • Enabling a sustainable future," n.d.) has caused the current era of geological history to be known as the "Plasticene" or the "Age of Plastic" (Zalasiewicz et al., 2016). In 2022, global plastic production almost reached 400.3 million tons ("Plastics the fast facts 2023 : A review on plastic contributions to European economy," 2023) out of which 50% are single-use plastic items (*Plastic Pollution Facts | PlasticOceans.org/the-facts*, accessed 31 October 2023). Moreover, the COVID-19 pandemic has exacerbated this pollution problem (Masud et al., 2023). Plastic waste has been recognized as ubiquitous in aquatic (marine and freshwater), terrestrial, and atmospheric environmental compartments, being relatively nonbiodegradable, and widely distributed in different ecosystems of our planet (Amobonye et al., 2021). Microplastics and nanoplastics (MNPs), miniaturized products of plastic materials, are currently a major health and environmental concern. MNPs are either directly manufactured (primary MNPs), intentionally added to medicines, cosmetics, and other personal care products, or derived from the fragmentation of larger plastics over time (secondary MNPs) (Amobonye et al., 2021). MNPs debris in water bodies (most of studies have concentrated on aquatic habitats) is composed mainly of different types of plastics, including polyethylene (PE), polypropylene (PP), polystyrene (PS), and polyvinyl chloride (PVC), which interact with organic matter, inorganic elements, and microorganisms (Mammo et al., 2020), in additionto being able to adsorb different toxic chemicals (Wu et al., 2019; Yuan et al., 2020).

Although there are various classifications, the International Organization for Standardization (*ISO/TR 21960:2020*) defines microplastics (MPs) as any solid, water-insoluble plastic particle with any dimension between 1 µm and 1 mm, and nanoplastics (NPs) have been defined as particles < 1 µm. A major concern for nanomaterials is their size, as it plays a decisive role in imparting toxicity to human and environmental health. Thus, a new research trend line has developed that supports that the plastic size *makes the poison* (negative impacts)

(Malinowska et al., 2023, 2022; Stapleton, 2019). It has been demonstrated that smaller NPs have a higher probability of gaining entrance and accumulating in different cells and tissues, which subsequently affect their physiological activities (Banerjee et al., 2021; Forte et al., 2016; Xie et al., 2023). Humans can absorb considerable amounts (approximately 203-312 particles/day) of MPs from the environment daily through food ingestion and other routes such as inhalation and dermal exposure (Cox et al., 2019). Even though, to date, the detection of NPs in human matrices is a challenge that has not been achieved for technical reasons, MPs have been reported in human blood, lung tissue, gastrointestinal tract, placenta, meconium, and breast milk (Gruber et al., 2022; Jenner et al., 2022; Leslie et al., 2022; Liu et al., 2023; Ragusa et al., 2021; Schwabl et al., 2019). In addition, different models, both *in vitro* and *in vivo*, have shown the ability of NPs to cross biological barriers (Deville et al., 2015; Hwang et al., 2022; Peng et al., 2020; Walczak et al., 2015) including the blood-brain barrier (Shan et al., 2022).

In Das et al.'s and co-workers' compilation of relevant toxicity studies of NPs and MPs (Das et al., 2021) the evidence indicated that size-dependent toxicity and oxidative stress were common findings in the included studies. Compared with MPs, studies on NPs are very few, and the results are inconclusive as to the dependence of effects on size and concentration, mainly due to disparity of experimental designs and possibly NP aggregation in test medium (Alimi et al., 2018; Torres-Ruiz et al., 2021).The effects of NPs have been studies for different target system in animal models (Song et al., 2009) (Rafiee et al., 2018) (Pitt et al., 2018), and also, more recently in nervous system (Shan et al., 2022), proving that exposure to plastic nanoparticles can cause behavioural changes and even brain abnormalities in zebrafish and mice (Torres-Ruiz *et al.*, 2021; Jeong *et al.*, 2022; Guimarães *et al.*, 2023; Torres-Ruiz *et al.*, 2023). *In vitro* experiments with NPS have mainly used epithelial cells and macrophages (Xie et al., 2023).

Thus, assessing the effects of NPs on cells of the nervous system is a critical knowledge gap, as infants and young children are more vulnerable than adults because the brain are still developing. Moreover, early life exposures may occur via the placenta, breastfeeding, and infant formula, as well as from feeding bottles, plastic toys, and other environmental sources (Song et al., 2021). Human neural stem cells (NSCs) provide an opportunity to study the effect of toxics in the early stages of neuronal development. These cells proliferate *in vitro* and can differentiate into mature neurons and glia. Therefore, they offer the possibility to study key endpoints of nervous system development. The present study was designed to use long-term propagated human NSCs, particularly hNS1 cell line, a clonal and multipotent stem cell line derived from the telencephalic region of the developing human brain. This hNS1 cell line has been successfully

used in other neurotoxicity experiments as well as in disease models (Coronel et al., 2018; González-Sánchez et al., 2015; Sandoval et al., 2019; Tanvig et al., 2009)

Polystyrene (PS) is a hardly biodegradable aromatic compound formed by polymerization of styrene monomers. It is one of the most widely produced plastic types (Kik et al., 2020; Maul et al., 2007), making it an environmental pollutant of increasing concern (Kwon et al., 2014).. In the present work, we use polystyrene nanoplastics (PS-NPs) to study the interactions between NPs and human NSCs, as a model of developmental neurotoxicity. PS-NPs have been widely used due to their commercial availability in several sizes and both with and without fluorescent labeling, which facilitates their localization in cells. Throughout the following study, we analyzed the penetration of 30-nm PS-NPs into the selected nervous system cellular model, their accumulation, and the subcellular localization of these nanoparticles within the cell. In addition, another objective is to evaluate the effects of different concentrations of PS-NPs on cell death and cell proliferation. As well as their involvement in the development of human NSC to neurons or glia, using β-Tubulin III, as a marker that is expressed in neurons and plays a role in neuronal functions such as axon guidance and intracellular transport, and GFAP, as an astrocyte marker involved in reactive astrocytosis, white matter maintenance and neuron-glia interactions.

2. MATERIAL AND METHODS

2.1 Nanoplastics characterization

PS-NPs solutions in cell medium were characterized by transmission electron microscopy (FEC Tecnai 12 operated at 120 kV). Before observation samples were sonicated (5 min), incubated on copper grids (10 min), washed with MQH_2O and dyed with 2% uranyl acetate. In addition, nanoparticle tracking analysis (NTA) was used to characterize PS-NPs solutions in order to evaluate particle size distribution in cell medium. For this, we employed a high sensitivity sCMOS camera on the NanoSight NS3000 (Malvern Instruments GmbH, United Kingdom), introducing samples automatically and recording 30 s movies at 30 frames per second. Three replicates for each PS-NPs concentration (0.5, 2.5, and 10 mg/L) were analyzed using the Software NTA 3.0. Particle z potential in cell culture medium was calculated in three replicates using the Zetasizer Nano (Malvern Instruments GmbH, United Kingdom).

2.2 Cell culture

We used hNS1 cell line, a model of human NSCs that has been previously characterized (Liste *et al*. 2004; Liste *et al.*, 2007; Coronel *et al.*, 2018; Sandoval *et al.*, 2019). This cell line is

non-transformed, derived from human fetal forebrain and immortalized with *v-myc* (Villa et al., 2000). Cells were cultured on poly-L-lysine (10 µg/mL; Sigma) coated plastic plates and proliferated in human stem cell (HSC) medium [Dulbecco's Modified Eagle Medium (DMEM)/F12 with GlutaMAX-I medium (Gibco) containing 0.26% AlbumaMAX (Gibco), 0.6% glucose (Merck), N2 Supplement 1× (Gibco), 5 mM HEPES (Gibco), penicillin/ streptomycin 1× (P/S; Lonza), non-essential aminoacids 1× (Gibco)] and supplemented with 20 ng/mL epidermal growth factor (EGF; PeproTech) and 20 ng/mL basic fibroblast growth factor (FGF2; PeproTech). hNS1 cells were differentiated by withdrawal of growth factors (EGF and FGF2) and addition of 0.5% heat-inactivated fetal bovine serum (FBS) (Biological Industries). Cells were kept in an incubator set to 37°C and 5% CO_2 (Heraus/HeraCell).

Prior to exposure to NPs, the hNS1 line was characterized at different days under differentiation conditions by immunocytochemistry to ensure stability and multipotency.

2.3 Polystyrene nanoplastics treatment

Fluorescently labelled (Firefli™ Fluorescent Green) and pristine polystyrene particles with a mean diameter of 30 nm were purchased from Fisher Scientific (Madrid, Spain), catalogue number Thermo Scientific™ G25 and 5003A respectively. PS-NPs of 1.05 g/cm³ density were provided as a 1% and 10% solution in water respectively, both with < 2% surfactant (SDS) to prevent agglomeration, and < 0.05% of the antibacterial agent NaN_3 (only fluorescently labelled particles). Cell cultures of hNS1 were treated with PS-NPs at 2 days after seeding. The stock solution was shaken and sonicated for 10 min before utilization. The PS-NPs were diluted in differentiation medium at 0.5, 2.5, and 10 µg/mL concentrations, and cells were differentiated 1 day for transmission electron microscopy (TEM) observation and 4 days for immunocytochemistry analysis.

In a second time-course experiment, the hNS1 cells were differentiated for 1, 2 or 4 days under exposure to PS-NPs at 2.5 µg/mL using TEM, to explore the effect of PS-NPs over time in the early stages of differentiation.

In all experiments, cell cultures not treated with PS-NPs were used as negative controls.

2.4 Immunocytochemistry

hNS1 cells treated with pristine PS-NPs for 4 days were rinsed with PBS and fixed in 4% paraformaldehyde for 10 min at room temperature (RT). Cultures were permeabilized with 0.25% Triton X-100 in PBS 1X incubated overnight at 4 °C with mouse monoclonal antibodies against β-tubulin III (1:1000; Biolegend #801202), Vimentin (1:1000; Santa Cruz Biotechnologies #sc-6260), and human Glial fibrillary acidic protein (GFAP) (1:1000; BD Pharmigen #556327), or

rabbit antibodies against Ki67 (1:500; Thermo Scientific #MA5-14520), and Caspase-3 (1:500; Cell Signaling #9664).

After removal of primary antibodies, cells were rinsed with PBS 1X and incubated with the corresponding secondary antibodies: Alexa 488 donkey antirabbit (1:500; Invitrogen #A21206), Alexa 488 donkey antimouse (1:500; Invitrogen #A21202), Alexa 555 donkey anti-rabbit (1:500; Invitrogen #A31572) and Alexa 555 donkey anti-mouse (1:500; Invitrogen #A31570). Cell nuclei were counterstained with Hoechst 33258 (Molecular Probes, Eugene, OR, USA) diluted in PBS (1:1000) for 10 min at RT. Pyknotic nuclei (small, condensed nuclei), characteristic of apoptotic cells, were also analyzed and quantified.

Analyses and photographs of fluorescent-immunostained cultures were carried out in an inverted Leica (Nussloch, Germany) DMi8 microscope equipped with a digital monochromatic camera (Leica K5). In all experiments, digital images were captured using Leica LASX software. Image analysis was performed using Photoshop CS6 Extended after randomly capturing at least 5 separate fields per well, with a minimum of three wells per experimental condition.

2.5 RNA isolation and reverse transcription PCR

Total RNA was isolated with the RNeasy Mini extraction kit (Qiagen, Valencia, CA, USA) according to manufacturer's instructions and treated with DNAses to avoid amplification of undesired genomic DNA. RNA concentration was quantified using TECAN INFINITE M200 plate reader (Tecan, Männedorf, Switzerland). The ratio of absorbance 260/280 nm was used to assess the purity of RNA and 1 µg of total RNA was reverse-transcribed in a reaction mixture using SuperScriptIII-RT (Life Technologies, Carlsbad, CA, USA) following the subsequent thermal profile: 25 °C 10 min; 50 °C 60 min; 75 °C 10 min.

Relative expression of cDNA was analyzed by quantitative real time PCR (q-RT-PCR) using the PowerUp SYBR Green Master Mix (Applied Biosystems, #A25742). 10 ng of total cDNA and 10 µM of primers were used in a 15 µL reaction mixture. q-RT-PCRs were performed using primers for the corresponding human target genes.

Table 1. Primer pairs and sequences

Gene	Forward Primer Sequence	Reverse Primer Sequence
TUBB3	5'-GCAACTACGTGGGCGACT-3'	5'-ATGGCTCGAGGCACGTACT-3'

GFAP	5'-GTTCTTGAGGAAGATCCACGA-3'	5'-CTTGGCCACGTCAAGCTC-3'
MKI67	5'-TGACCCTGATGAGAAAGCTCAA-3'	5'-CCCTGAGCAACACTGTCTTTT-3'
VIM	5'-TGGTCTAACGGTTTCCCCTA-3'	5'-GACCTCGGAGCGAGAGTG-3'
BAX	5'-AGCAAACTGGTGCTCAAGG-3'	5'-CTTGGATCCAGCCCAACA-3'
BCL2	5'-TTGACAGAGGATCATGCTGTACT-3'	5'-ATCTTTATTTCATGAGGCACGTT-3'
Housekeeping gene *TBP*	5'-GAGCTGTGATGTGAAGTTTCC-3'	5'-TCTGGGTTTGATCATTCTGTAG-3'

The Applied Biosystems QuantStudio 3 Real-Time PCR System was used to determine the relative expression of target mRNA in each sample, estimated by the $2^{-\Delta\Delta Ct}$ relative quantification method. Gene expression levels were normalized against *TBP* levels in each sample. To analyze q-RT-PCR data two replicates for each gene of interest under each exposure concentration were measured in three independent experiments.

2.6 Transmission Electron Microscopy (TEM)

hNS1 cells treated with pristine PS-NPs were cultured as monolayers adhered to glasses coverslips of 12 mm diameter using poly-L-lysine (10 µg/ml; Sigma). At specific times the cells were rinsed with PBS 1X and fixed with 2.5% glutaraldehyde, and 2% paraformaldehyde (PFA) in 0.1M Na_2HPO_4/$NaHPO_4$, pH 7.4 for 1h at RT. The monolayers were then washed with 0.1M Na_2HPO_4/$NaHPO_4$ buffer, pH 7.4, postfixed with 1% osmium tetroxide and 1% potassium ferricyanide for 1h at 4 °C. Cells were treated with 0.15% tannic acid in 0.1M Na_2HPO_4/ $NaHPO_4$ buffer, pH 7.4, for 1 min and stained with 1% uranyl acetate for 1h at RT. The samples were subsequently dehydrated at 4 °C using increasing concentrations of ethanol (50, 75, 95% for 10 min each and two times 100% for 30 min each). The monolayers were infiltrated with increasing concentrations of epoxy resin (50% and 100%) and polymerised using gelatine capsules of 5 mm diameter, at 60 °C for 48h. Cell monolayers were cut into ultrathin sections (50-70 nm) with a diamond-knife on a Leica UC6 ultramicrotome and deposited on Formvar-coated copper grids. The sections were stained with saturated uranyl acetate under humid conditions, followed by 2% Reynold´s lead citrate. A Tecnai 12 electron microscope operated at 120 kV was used to visualise the samples and images were recorded with a CCD (Charged Coupled Device) FEI Ceta camera.

2.7 Statistical analysis

Statistical tests were completed using Graphpad Prism 9.1.2. Results are shown as the mean ± standard errors (S.E.M.) of data from 3 independent experiments (n=3). Mean values were compared using the one-way ANOVA for multiple comparison followed by the Dunnet or Tukey post hoc test when significant differences occurred between groups. *p* values < 0.05 were considered to be statistically significant (*p < 0.05, **p < 0.01, ***p < 0.001, ****p < 0.0001).

3. RESULTS

3.1 PS-NPs characterization

PS-NPs observed with TEM have a particle size of 25 ± 0.6 nm according to manufacturer's specifications (Fig.1E). However, PS-NPs were observed in aggregates at all concentrations, although sonication was performed prior to use. Particle aggregation was also evident in results of NTA analysis. The mean aggregate size changed depending on PS-NPs concentration: 112.4 ± 37.5 nm (0.5 µg/mL), 112.0 ± 44.2 nm (2.5 µg/mL), and 115.5 ± 43.9 nm (10 µg/mL) (Fig. 1A-C). The results of DLS assays show that the z potential was negative and similar at all concentrations: −25.4 ± 1.06 mV (0.5 µg/mL), −33.8 ± 1.30 mV (2.5 µg/mL), and –33.95 ± 0.64 mV (10 µg/mL) (Fig. 1).

3.2 PS-NPs internalization

In a preliminary experiment, cells were exposed to fluorescently labelled PS-NPs concentrations of 10 µg/mL, 25 µg/mL and 50 µg/mL and for short exposure times (16h, 24h and 48h). Under these conditions, it could be observed that PS-NPs appeared to be able to enter the cells. Fluorescence was maintained at all exposure times. With Hoechst staining (blue nuclei) PS-NPs were not detected in the nucleus but remained in the cytoplasm of the cell (Supplementary information Fig.1S).

After verifying that the PS-NPs appeared capable of entering our test system (hNS1 cell line), a wide range of concentrations and exposure times was employed to establish the optimal conditions for subsequent assays. The results of fluorescence microscopy demonstrated that at the fourth day of differentiation, there was a highest amount of fluorescence in the cell interior, and especially at higher concentrations, there was a marked increase in the aggregation of the PS-NPs inside the cell. There also appeared to be a loss of hNS1 morphology with respect to their corresponding differentiation stage (Supplementary information Fig.1S, 2S). For the remaining

247 experiments, we selected concentrations of 0.5 µg/mL, 2.5 µg/mL, and 10 µg/mL and exposure
248 times of 1 to 4 days in differentiation without medium renewal.

249 In a first experiment, to accurately observe the internalisation of PS-NPs, differentiated
250 and 24h treated cells (control and three selected concentrations) were fixed and processed for
251 electron microscopy. As shown in Figure 2, PS-NPs aggregated in the intercellular spaces and
252 remained adjacent to the plasma membrane at all concentrations tested, and at the highest
253 concentration (10 µg/mL) these aggregates were higher (Fig. 2C, D). In addition, cells treated
254 with 0.5 and 2.5 µg/mL PS-NPs show clathrin coated pits at the plasma membrane that contain
255 PS-NPs (Fig. 3).

256 In this context, Figure 4 shows the presence of internal vesicles and vacuoles containing
257 PS-NP particles, indicating that PS-NPs are already taken up by hNS1 cells within 24 h. Among
258 the various cytosolic compartments containing PS-NPs, early endosomal vacuoles with their
259 characteristic flat clathrin coat were observed. With increasing PS-NPs concentration,
260 accumulations of them were observed in the lumen of larger vacuoles.

261 In the time course-study, when cells were exposed to 2.5 µg/mL of PS-NPs we observed
262 that the particles were inside vacuoles (Fig. 5A) from day 1 of differentiation. After 4 days of
263 differentiation, these vacuoles included other structures, in addition to the incorporated PS-NPs
264 (Fig. 5B). With increasing exposure time, the accumulating PS-NPs structures became larger and
265 more electron dense. Interestingly, as exposure time increased, we observed protrusions of the
266 plasma membrane that were often juxtaposed to vacuoles containing PS NPs, some of them
267 surrounded by Endoplasmic Reticulum cisterna (Fig. 6).

268 **3.3 Effect of PS-NPs on cell death and cell proliferation**

269 To determine whether the apparent changes in cell morphology were due to cell death
270 and the corresponding apoptotic mechanisms, a monoclonal antibody against caspase 3 was
271 used. Caspase 3 detects endogenous levels of the large fragment (17/19 kDa) of activated
272 caspase 3, whose activation plays a key role in apoptosis. A dose-dependent increase in Caspase
273 3 activation was observed: control, 6.68 ± 0.79 %; 0.5 µg/mL, 10.72 ± 1.21 %; 2.5 µg/mL, 14.26
274 ± 1.30 %; 10 µg/mL, 15.75 ± 0.85 % (Fig. 7B), being significant at all concentrations tested. This
275 increase in apoptosis after treatment with PS-NPs also appears to be confirmed by qRT-PCR
276 (ratio BAX/BCL-2), but statistical significance was only observed at the 2.5 µg/mL dose (Fig. 7C).
277 BCL-2 and BAX are two discrete members of a gene family involved in the regulation of cellular
278 apoptosis a cell with a high BAX/BCL-2 ratio will be more sensitive to apoptotic stimuli. In
279 addition, we have also analyzed and quantified the percentage of pyknotic nuclei that are

characteristic of apoptotic cells. A dose-dependent increase in the percentage of pyknotic nuclei was observed: control, 6.60 ± 0.23 %; 0.5 µg/mL, 10.33 ± 0.24 %; 2.5 µg/mL, 12.90 ± 0.15 %; 10 µg/mL, 17.40 ± 0.81 % (Supplementary information Fig.4S). The increasing levels of cell death and the toxic effect observed in hNS1 cells reflect the cytotoxicity of PS-NPs at high concentrations and extended exposures.

To assess the possible effects of PS-NPs in cell proliferation, we evaluated the expression of Ki67 by ICC at protein level (Fig. 7B) and by qRT-PCR at the gene expression level (Fig. 7C). Ki-67 is a key cell proliferation marker (universally expressed among cells in the G1, S, and G2 phases). In the case of Ki-67, the results show a dose-dependent decrease (Control: 27.09 ± 1.42%; 0.5 µg/mL: 24.24.67 ± 1.16%; 2.50 µg/mL: 24.45 ± 1.15%, 10 µg/mL: 21.50 ± 1.31%), statistically significant at all concentrations used. A similar trend, although statistically significant only at the highest dose, was observed when gene expression levels for MKi67 were determined.To study the effect of PS-NPs in neural precursors, a monoclonal antibody against Vimentin was employed (Fig. 7). For this marker, no changes were observed after treatment with PS-NPs at any of the concentrations used at either the protein (control, 91.50 ± 1.07%, 0.5 µg/mL, 91.68 ±0.90%, 2.5 µg/mL, 90.00 ± 0.89%, 10 µg/mL, 91.25 ± 0.89%) or mRNA level.

3.4 Effects of PS-NPs in cell differentiation of hNS1 cells

To assess if PS NPs affect the cell fate specification of hNS1 cells, antibodies against β-tubulin III (neuronal marker) and GFAP (astrocyte marker) were used (Fig. 8).A slight decreasing trend in the percentage of ß-III-tubulin positive cells was observed as the concentration of PS-NPs increased, (control, 35.06 ± 1.12%, 0.5 µg/mL, 34.11 ± 1.37%, 2.5 µg/mL, 31.29 ± 1.18%, 10 µg/mL, 30.48 ± 1.24 %) (Fig. 8B), which became statistically significant only at the highest concentration. The same trend of decreased *TUBB3* expression was observed at all doses tested (Fig. 8C).In the case of GFAP, no changes were observed in the percentage of labelled positive cells due to PS-NP treatment (Control: 68.28 ± 2.99; 0.5 µg/mL: 62.13 ± 2.65 %; 2.5 µg/mL: 66.02 ± 2.15 %; 10 µg/mL: 69.57 ± 2.38 %), although interestingly *GFAP* gene expression was decreased with respect to the control at all dose levels tested.

4. DISCUSION

4.1 PS-NPs characterization and suitability of the test system

There are undeniable technical difficulties in analyzing and characterizing nanoplastics, so the techniques used to analyze other nanomaterials, such as nanoparticle tracking analysis (NTA), dynamic light scattering (DLS), or transmission electron microscopy (TEM) (Das et al.,

2021), used in our study, are very useful to verify both the size and distribution of PS-NPs in the culture medium and cellular systems. One problem in most research on the toxicity of NP is to mimic the natural behaviour of NPs when they spread in different matrices (water, culture media, etc.). In our work, sonication failed to prevent aggregation of particles in all concentrations examined, although visualization of PS-NPs by TEM showed that the size of individual particles was consistent with commercial standards, and most aggregates stayed in the nano-range (around 100nm) (Fig.1). The z-potential of PS-NPs in the DLS test is between -25 and -30 mV, indicating that the surface charge of the particles remains constant regardless of the concentration. These NPs are anionic and moderately stable (McNeil, 2011), which is consistent with the low aggregation observed.To avoid possible hazardous synergistic effects, we did not use chemical agents such as detergents to prevent aggregation. Agglomeration of particles may alter their toxicity, but this condition may be better suited to simulate natural dispersions in the environment (Alimi et al., 2018; Lins et al., 2022). Even though various techniques like sonication and the use of surfactant agents have been tried in other works (Eitzen et al., 2020), agglomerated particles are likely to appear again over time (Bruinink et al., 2015). Moreover, when inside the biological model system, tissue-specific agglomerations and de-agglomerations might take place that could alter distribution, toxicity, and clearance time. Furthermore, distinct agglomeration patterns may be the reason for the observed lack of correlation between PS-NP particle size and degree of toxicity in previous studies (Torres-Ruiz et al., 2021).

4.2 PS-NPs entrance mechanisms and accumulation

Understanding the uptake of NPs in cells of the nervous system will help to understand their potential effects in humans and our study is the first to show a potential entrance mechanism into these types of cells. It is reported that the most common mechanism by which nanoparticles enter cells is endocytosis, an energy-dependent process, that takes up substance from the extracellular environment by vesicles generated from the cell plasma membrane (Doherty and McMahon, 2009). There are different mechanisms of endocytosis mainly phagocytosis (barely used as mechanism for NPs uptake), micropinocytosis, and receptor-mediated endocytosis (RME). Fluid phase uptake by clathrin mediated endocytosis into the cell is compatible with what is shown in our electron microscopy images (Fig. 3), where we were able to detect the PS-NPs inside clathrin coated pits at the plasma membrane and inside the cell in early endosomes containing PS-NPs, the size of the observed structures is consistent with that described in the scientific literature (Liu et al., 2021; McMahon and Boucrot, 2011). When the vesicle is internalized, it loses its clathrin coat and fuses with other vesicles to form an early

endosome that turns into a late endosome that fuses with a lysosome, similarly to what has been observed in other cell types (Popova et al., 2013; Sachse et al., 2002). Previous works, using different cell models, have shown that nanoparticles up to 150 nm in size are internalized mainly via clathrin/caveolin mediated endocytosis (CME, CVME) (Foroozandeh and Aziz, 2018; Liu et al., 2021; Yang and Wang, 2023), but CME seems to be most common, especially for PS-NPs (Kannan et al., 2014; Wang et al., 2017), whereas larger particles are taken up by micropinocytosis (Liu et al., 2021). Another study, with similar PS-NPs and using human gastric adenocarcinoma cells (Forte et al., 2016), confirmed that CME is the preferred endocytic pathway during internalization. It is possible that endocytic mechanisms of NP entry might depend on NP type, size and specially cell type. Therefore, further work is needed to characterize this important first step in NPs toxicity.

In a recent article (Liu et al., 2022), the interaction of PS-NPs with sizes of 50 and 100 nm was studied in two types of human lung cells. The authors concluded that the lysosome was the main organelle in which both PS-NPs accumulated in cells, and furthermore, the 50nm PS-NPs were distributed around the plasma membrane in both cell types. Exposure of intestinal Caco-2 cells to higher concentrations of PS-NPs (50-100 μg/mL) than those used in this study resulted in increased accumulation of lysosomes and electron-dense vesicles in the cytoplasm and increased inflammation of mitochondrial cristae (Cortés et al., 2020). Moreover, the accumulation of lysosomes was also been observed in zebrafish cells (Yang and Wang, 2023). This could support our findings where 30 nm PS-NPs are observed close to the plasma membrane and are also detected within hNS1 in early endosome-like structures and at longer exposure times or at higher concentrations in lysosome-like organelles.

As exposure time increased, plasma membrane protrusions could be observed (Fig. 6). Interestingly, these protusions were often juxtaposed to large vacuoles with numerous NPs in their lumen. Future experiments will determine whether these protrusions are connected to the vacuoles and could provide a pathway for the cell to clear the NPs.

4.3 PS-NPs Toxicity

The available studies on the interaction between PS-NPs and human cells have mainly focused on their cytotoxicity (Kim et al., 2022; Liu et al., 2015; Sarma et al., 2022; Shi et al., 2022; Weber et al., 2022; Zhang et al., 2022). Some of these studies have also shown that PS-NPs can produce reactive oxygen species (Sarma *et al.*, 2022; Zhang *et al.*, 2022), trigger a range of inflammatory responses (Forte et al., 2016; Weber et al., 2022), and reduce cell viability (Forte et al., 2016; Shi et al., 2022). However, no assays have been performed with human NSCs to

investigate the effect of PS-NPs on the early stages of neural development. In this work, we studied the effects of different concentrations of PS-NPs on cell death, proliferation, and cell fate specification under differentiation conditions using the hNS1 neural cell line, showing that PS-PNs dose-dependently increase apoptosis, decrease cell proliferation and differentiation to neurons at the highest dose tested. Despite the limited information on the effects of NPs on the nervous system, behavioural changes have been observed in mice following oral PS-NPs exposure (Rafiee et al., 2018).

Brain development is a highly coordinated and complex process that occurs in both the gestational and postnatal periods and is characterized by multiple biological processes (Rosca et al., 2020). Disruptions of any of these neurodevelopmental processes are described as common key events (KE) in a network of adverse outcome pathways (AOP) for human neurotoxicity leading to the same adverse outcome (AO) (i.e., learning and memory disorders in children) (https://aopwiki.org/, ID: 54, 42, 134,12, 13). Currently, it is possible to study some of these KE by *in vitro* assays with immortalized human NSC cell lines, which offer several advantages. First, they represent a homogeneous cell population of human origin, maintain a stable phenotype over time, and are easily differentiated into a mixed culture of neurons and glial cells. In addition, they provide an unlimited supply of neural precursors, neurons and glial cells. One of these immortalized cell lines is the hNS1 used in our study, that provides a suitable *in vitro* system for modelling early stages of neurodevelopment.

Apoptosis is involved in cell turnover, physiological involution, and atrophy of various tissues and organs (Kerr et al., 1972). In the current work, we observed that PS-NPs induced cell death in hNS1 during the differentiation process, the results suggest that apoptosis is induced through the intrinsic pathway evidenced by an increase in pyknotic nuclei, activated caspase 3 and Bax/Bcl2 ratio. In KEGG (https://www.genome.jp/kegg/) it has been confirmed that Caspase 3, Bax and Bcl2 belong to the intrinsic apoptotic pathway hsa04215 and in terms of Gene Ontology BAX and BCL2 are associated with the apoptotic process GO:0006915 and CASP3 and BCL2 are associated with the term GO:0010623 programmed cell death in cell development. It is well known that chemical induced cell death alters the integration and transmission of information through neural networks, thus providing the basis for the subsequent deterioration of learning and memory. Similar sized PS-NPs have also induced apoptosis and inflammation in A549 cells, a human lung carcinoma epithelial cell line (Halimu et al., 2022). With larger PS NPs (50nm), cell death has also been reported in mouse epithelial cells and human hepatocellular carcinoma (HepG2) (He et al., 2020; Liang et al., 2021). In addition to this increase in cell death, we observed a decrease in cell proliferation, with no change in the expression of neural

precursors. The decreased cell proliferation, an ATP-dependent process, has been linked to abnormal growth-factor signalling and cellular energy depletion (DeBerardinis et al., 2008).

Regarding phenotypic specification, there is no previous information on the effects of nanoplastic on human NSC or mixed cultures of neurons and glia. Our assay showed that neural differentition decreased slighly, but only at the highest concentration tested, whereas no changes were observed in glial specification. The direct relationship between alterations in neural network function and specific cognitive deficits is difficult to establish given the many forms that learning and memory can take and the complexity of synaptic interactions in even the simplest brain circuit. Coculture systems provide a more comprehensive developmental neurotoxicity assessment (Rosca et al., 2023), as perturbations in a single cell type may not represent all the effects on the onset and/or progression of neural disorders by environmental chemicals (Liang et al., 2019). For example, abnormal interactions between neurons and glial cells are a major cause of neural disorders (Meyer and Kaspar, 2017; Rahman et al., 2022).

It has been described (Dekkers et al., 2013) that under physiological conditions, components of the apoptotic machinery in the developing brain regulate synapse formation and neuronal connectivity. Therefore, PS-NPs act as a stressor that increases the number of apoptotic cells. This is a KE that has a negative effect on synaptogenesis. In addition, PS-NPs reduces the number of cells that divide and has negative effects on differentiation to the neural phenotype, which means that there could be fewer axons to establish synaptic contacts (Olney, 2014). All the above mechanisms could contribute to a reduction in synaptogenesis and neuronal networks formation, which could affect normal neurodevelopment.

5. CONCLUSION

Our results deepen the understanding of the interaction and effects of PS-NPs on neural stem cells. PS-NPs were able to enter the cell without being detected in the nucleus at all concentrations tested and localized in early endosomes and accumulated in vacuoles. The latter became larger with increasing exposure time and concentration, together with obvious changes in the overall morphology of hNS1 cells.

Exposure to PS-NPs resulted in a dose-dependent activation of caspase-3, suggesting that they were producing apoptotic death. In addition, a decrease in cell proliferation was observed at the highest dose tested, with no change in neural precursor expression. With respect to cell differentiation, a slight decrease in neural differentiation was observed, also at the highest dose, while no changes in glial specification were evident at the protein level. If the

446 described changes of our *in vitro* system are taking place *in vivo* as well, they could lead to
447 deficient synaptogenesis and abnormal neural network in early stages of brain development.
448 Considering the widespread presence of nanoplastics in the environment and their ability to
449 enter humans by different routes and cross the placental and blood-brain barrier, our study has
450 demonstrated that PS-NPs, even when forming aggregates in the culture medium, are able to
451 enter and accumulate in neural stem cells and induce toxic effects at very early stages of
452 differentiation. Therefore, it is crucial to further investigate their mechanisms of action and their
453 potential health effects, especially considering the association of these pollutants with
454 important diseases whose incidence has increased in recent years, such as autistic or
455 hyperactivity disorders, anxiety, depression and neurodegenerative processes, to name but a
456 few.

457 **Conflict of interest**

458 The authors declare that they have no conflicts of interest.

459 **Funding**

460 This work was supported by the project "Use of alternative methods for the evaluation
461 of the effects of nanoplastics on neurodevelopment" funded by IMIENS. It was also partially
462 supported by Grant No. PID2021-126715OB-I00 from MCIN/AEI/10.13039/ 410 501100011033
463 and by "ERDF A way of making Europe" and by the Instituto de Salud Carlos III 411 (ISCIII) Grant
464 AESI, PI22CIII/00055.

465

466 **Acknowledgements**

467 The authors are grateful for the support and contribution to the initial stages of the work
468 of the undergraduate and master's degree students who have been in our laboratories.

469

Figure Legends

Figure 1: Polystyrene Nanoplastic (PS-NPs) characterization. Samples were analyzed in cell medium containing 0.5 (A), 2.5 (B), and 10.0 (C) µg/mL of PS-NP. NanoSight NS300 (Malvern Instruments Ltd) was used to measure aggregated particle size distribution(A-D), and Zetasizer Nano SZ (Malvern Instruments Ltd) for Zeta potential (D). PS-NPs in cell medium observed under transmission electron microscopy confirms an individual particle size of approx. 30 nm (consistent with commercial standards) but aggregates of around 100 nm (red circle) (E).

Figure 2: Intercellular space, hNS1 cells exposed to 30nm PS-NPs for 24h. A and B) PS-NPs (at 0.5 µg/mL) aggregated in the intercellular space and close to the plasma membrane, the dotted line shows the area where the PS-NPs are grouped. The black arrowheads show individual PS-NPs. C and D) At 10 µg/mL PS-NPs increased aggregation of nanoparticles. Scale bar 500 nm. p – plasma membrane; n – nucleus; m – mitochondria.

Figure 3: Membrane invaginations surrounding PS-NPs. hNS1 cells exposed to 30nm PS-NPs for 24h at 2.5µg/mL. Arrows point to clathrin coated pits. The black arrowheads show PS-NPs in the intercellular space and the white arrowhead shows PS-NPs in a clathrin-coated pit. A) Scale bar 500 nm (insert in A Scale bar 200 nm). B) Scale bar 200nm. p – plasma membrane; n – nucleus; m – mitochondria.

Figure 4: Cytoplasmic compartments containing PS-NPs. A) and B) Endocytic vesicle and early endosomal vacuole, respectively, with a cluster of PS-NPs in the lumen (2.5 µg/mL for 1 day treatment). The arrow marks the characteristic flat clathrin coat, present on early endosomal vacuoles. Arrowheads show PS-NPs in the intercellular space. Scale bar 500nm (insert in A, Scale bar 200 nm). C) PS-NPs accumulates in vacuoles close to mitochondria (10 µg/mL for 1 day treatment). Scale bar 500nm. p – plasma membrane; m – mitochondria.

Figure 5: Time-course of PS-NP internalization. A) Nanoparticles inside a single membrane compartments/vacuole, hNS1 treated for 1 days at 2.5 µg/mL PS-NPs. B) hNS1 cells treated for 2 days at 2.5 µg/mL, structures containing PS-NPs accumulations increased in size and contain internal vesicles/membranes (arrowheads). C and D) hNS1 cells treated for 4 days at 2.5 µg/mL PS-NP containing vacuoles have increased in size and contain electron dense, amorph material in the lumen. Scale bar on main figures 500nm, scale bar on inserts 200nm. p – plasma membrane; m – mitochondria; n – nucleus.

Figure 6: Time-course assay. hNS1 treated for 4 days at 2.5 µg/mL PS-NPs. PS-NPs-containing vacuoles close to the plasma membrane with protrusions on the plasma membrane. Scale bar 200nm. P - plasma membrane.

Figure 7: Effect of PS-NPs on cell death and cell proliferation. A) Representative images immunocytochemistry for Caspase 3, Ki-67 and Vimentin counterstained with Hoechst. Scale bar = 50 µm. B) Percentage of positive cells for Caspase 3, Ki-67 and Vimentin with respect to total cells. C) Data represent mean ± S.D. (n = 3). Asterisks indicate significant differences (*p b 0.05;** p 0.01; ****p b 0.0001) in treated cells with respect to controls.

Figure 8: Effect of PS-NPs cell differentiation. A) Representative images immunocytochemistry for β- tubulin III and GFAP counterstained with Hoechst. Scale bar = 50 µm. B) Percentage of positive cells for β- tubulin III and GFAP with respect to total cells. Data represent mean ± S.D. (n = 3). C) Relative expression levels of TUBB3 and GFAP mRNA obtained by q-RT-PCR. Data represent mean and S.E. (n=3). Asterisks indicate significant differences (*p< 0.05; **p < 0.01; **** p < 0.001) in treated cells.

Figure 1S: Preliminary experiments. Representative images of hNS1 cells treated with 30 nm fluorescence-labelled PS-NPs at concentrations of 10, 25 and 50 µg/mL, for 16, 24 and 48 h in differentiation phase. Scale bar = 50 µm.

Figure 2S: Preliminary experiments. Representative images of hNS1 cells treated with 30 nm fluorescence-labelled PS-NPs at concentrations of 0.5, 2.5 and 10 µg/mL, for 1 and 4 days in differentiation phase. Scale bar = 50 µm.

Figure 3S: Overview of the hNS1 cells with a normal appearing nucleus, unaltered by apoptosis. Panels A (Scale bar 5um) and B (Scale bar 500nm) are the whole cell images of those corresponding to subpanel A in Figure 5 (hNS1 treated for 1 days at 2.5 µg/mL PS-NPs). Panels C (Scale bar 2um) and D (Scale bar 500nm) are the whole cell images of those corresponding to subpanel B in Figure 5 (hNS1 cells treated for 2 days at 2.5 µg/mL). pm – plasma membrane; m – mitochondria; n – nucleus; v - vacuole.

Figure 4S: Effect of PS-NPs on pyknotic nuclei. A) Representative images for pyknotic nuclei with Hoechst. Scale bar = 50 µm. Arrows indicate positive cells for pyknotic nuclei B) Percentage of positive cells for pyknotic nuclei with respect to total cells. Data represent mean ± S.D. (n = 3). C) Relative expression levels of TUBB3 and GFAP mRNA obtained by q-RT-PCR. Data represent mean and S.E. (n=3). Asterisks indicate significant differences (*p< 0.05; **p < 0.01; **** p < 0.001) in treated cells.

534 **REFERENCES**

535 Alimi, O.S., Farner Budarz, J., Hernandez, L.M., Tufenkji, N., 2018. Microplastics and
536 Nanoplastics in Aquatic Environments: Aggregation, Deposition, and Enhanced
537 Contaminant Transport. Environ. Sci. Technol. 52, 1704–1724.
538 https://doi.org/10.1021/ACS.EST.7B05559/ASSET/IMAGES/LARGE/ES-2017-
539 05559J_0004.JPEG

540 Amobonye, A., Bhagwat, P., Raveendran, S., Singh, S., Pillai, S., 2021. Environmental Impacts of
541 Microplastics and Nanoplastics: A Current Overview. Front. Microbiol. 12.
542 https://doi.org/10.3389/fmicb.2021.768297

543 Banerjee, A., Billey, L.O., Shelver, W.L., 2021. Uptake and toxicity of polystyrene
544 micro/nanoplastics in gastric cells: Effects of particle size and surface functionalization.
545 PLoS One 16, 1–25. https://doi.org/10.1371/journal.pone.0260803

546 Bruinink, A., Wang, J., Wick, P., 2015. Effect of particle agglomeration in nanotoxicology. Arch.
547 Toxicol. 89, 659–675. https://doi.org/10.1007/S00204-015-1460-6/METRICS

548 Coronel, R., Bernabeu-Zornoza, A., Palmer, C., Muñiz-Moreno, M., Zambrano, A., Cano, E.,
549 Liste, I., 2018. Role of Amyloid Precursor Protein (APP) and Its Derivatives in the Biology
550 and Cell Fate Specification of Neural Stem Cells. Mol. Neurobiol. 55, 7107–7117.
551 https://doi.org/10.1007/s12035-018-0914-2

552 Cortés, C., Domenech, J., Salazar, M., Pastor, S., Marcos, R., Hernández, A., 2020. Nanoplastics
553 as a potential environmental health factor: effects of polystyrene nanoparticles on
554 human intestinal epithelial Caco-2 cells. Environ. Sci. Nano 7, 272–285.
555 https://doi.org/10.1039/C9EN00523D

556 Cox, K.D., Covernton, G.A., Davies, H.L., Dower, J.F., Juanes, F., Dudas, S.E., 2019. Human
557 Consumption of Microplastics. Environ. Sci. Technol. 53, 7068–7074.
558 https://doi.org/10.1021/ACS.EST.9B01517

559 Das, R.K., Sanyal, D., Kumar, P., Pulicharla, R., Brar, S.K., 2021. Science-society-policy interface
560 for microplastic and nanoplastic: Environmental and biomedical aspects. Environ. Pollut.
561 290, 117985. https://doi.org/10.1016/j.envpol.2021.117985

562 DeBerardinis, R.J., Lum, J.J., Hatzivassiliou, G., Thompson, C.B., 2008. The biology of cancer:
563 metabolic reprogramming fuels cell growth and proliferation. Cell Metab. 7, 11–20.
564 https://doi.org/10.1016/J.CMET.2007.10.002

565 Dekkers, M.P.J., Nikoletopoulou, V., Barde, Y.A., 2013. Cell biology in neuroscience: Death of

566 developing neurons: new insights and implications for connectivity. J. Cell Biol. 203, 385–
567 393. https://doi.org/10.1083/JCB.201306136

568 Deville, S., Penjweini, R., Smisdom, N., Notelaers, K., Nelissen, I., Hooyberghs, J., Ameloot, M.,
569 2015. Intracellular dynamics and fate of polystyrene nanoparticles in A549 Lung epithelial
570 cells monitored by image (cross-) correlation spectroscopy and single particle tracking.
571 Biochim. Biophys. Acta - Mol. Cell Res. 1853, 2411–2419.
572 https://doi.org/10.1016/J.BBAMCR.2015.07.004

573 Doherty, G.J., McMahon, H.T., 2009. Mechanisms of endocytosis. Annu. Rev. Biochem. 78,
574 857–902. https://doi.org/10.1146/ANNUREV.BIOCHEM.78.081307.110540

575 Eitzen, L., Ruhl, A.S., Jekel, M., 2020. Particle Size and Pre-Treatment Effects on Polystyrene
576 Microplastic Settlement in Water: Implications for Environmental Behavior and
577 Ecotoxicological Tests. Water 2020, Vol. 12, Page 3436 12, 3436.
578 https://doi.org/10.3390/W12123436

579 Foroozandeh, P., Aziz, A.A., 2018. Insight into Cellular Uptake and Intracellular Trafficking of
580 Nanoparticles. Nanoscale Res. Lett. 13. https://doi.org/10.1186/S11671-018-2728-6

581 Forte, M., Iachetta, G., Tussellino, M., Carotenuto, R., Prisco, M., De Falco, M., Laforgia, V.,
582 Valiante, S., 2016. Polystyrene nanoparticles internalization in human gastric
583 adenocarcinoma cells. Toxicol. Vitr. 31, 126–136.
584 https://doi.org/10.1016/j.tiv.2015.11.006

585 González-Sánchez, H.M., Monsiváis-Urenda, A., Salazar-Aldrete, C.A., Hernández-Salinas, A.,
586 Noyola, D.E., Jiménez-Capdeville, M.E., Martínez-Serrano, A., Castillo, C.G., 2015. Effects
587 of cytomegalovirus infection in human neural precursor cells depend on their
588 differentiation state. J. Neurovirol. 21, 346–357. https://doi.org/10.1007/s13365-015-
589 0315-5

590 Gruber, E.S., Stadlbauer, V., Pichler, V., Resch-Fauster, K., Todorovic, A., Meisel, T.C.,
591 Trawoeger, S., Hollóczki, O., Turner, S.D., Wadsak, W., Vethaak, A.D., Kenner, L., 2022. To
592 Waste or Not to Waste: Questioning Potential Health Risks of Micro- and Nanoplastics
593 with a Focus on Their Ingestion and Potential Carcinogenicity. Expo. Heal.
594 https://doi.org/10.1007/s12403-022-00470-8

595 Guimarães, A.T.B., Freitas, Í.N., Mubarak, N.M., Rahman, M.M., Rodrigues, F.P., Rodrigues, A.S.
596 de L., Barceló, D., Islam, A.R.M.T., Malafaia, G., 2023. Exposure to polystyrene
597 nanoplastics induces an anxiolytic-like effect, changes in antipredator defensive

response, and DNA damage in Swiss mice. J. Hazard. Mater. 442, 130004. https://doi.org/10.1016/J.JHAZMAT.2022.130004

Halimu, G., Zhang, Q., Liu, L., Zhang, Z., Wang, X., Gu, W., Zhang, B., Dai, Y., Zhang, H., Zhang, C., Xu, M., 2022. Toxic effects of nanoplastics with different sizes and surface charges on epithelial-to-mesenchymal transition in A549 cells and the potential toxicological mechanism. J. Hazard. Mater. 430, 128485. https://doi.org/10.1016/J.JHAZMAT.2022.128485

He, Y., Li, J., Chen, J., Miao, X., Li, G., He, Q., Xu, H., Li, H., Wei, Y., 2020. Cytotoxic effects of polystyrene nanoplastics with different surface functionalization on human HepG2 cells. Sci. Total Environ. 723, 138180. https://doi.org/10.1016/J.SCITOTENV.2020.138180

Hwang, K.S., Son, Y., Kim, S.S., Shin, D.S., Lim, S.H., Yang, J.Y., Jeong, H.N., Lee, B.H., Bae, M.A., 2022. Size-Dependent Effects of Polystyrene Nanoparticles (PS-NPs) on Behaviors and Endogenous Neurochemicals in Zebrafish Larvae. Int. J. Mol. Sci. 23, 10682. https://doi.org/10.3390/IJMS231810682/S1

ISO/TR 21960:2020(en), Plastics — Environmental aspects — State of knowledge and methodologies [WWW Document], n.d. URL https://www.iso.org/obp/ui/#iso:std:iso:tr:21960:ed-1:v1:en (accessed 3.9.23).

Jenner, L.C., Rotchell, J.M., Bennett, R.T., Cowen, M., Tentzeris, V., Sadofsky, L.R., 2022. Detection of microplastics in human lung tissue using μFTIR spectroscopy. Sci. Total Environ. 831, 154907. https://doi.org/10.1016/J.SCITOTENV.2022.154907

Jeong, B., Baek, J.Y., Koo, J., Park, S., Ryu, Y.K., Kim, K.S., Zhang, S., Chung, C.H., Dogan, R., Choi, H.S., Um, D., Kim, T.K., Lee, W.S., Jeong, J., Shin, W.H., Lee, J.R., Kim, N.S., Lee, D.Y., 2022. Maternal exposure to polystyrene nanoplastics causes brain abnormalities in progeny. J. Hazard. Mater. 426. https://doi.org/10.1016/j.jhazmat.2021.127815

Kannan, R.M., Nance, E., Kannan, S., Tomalia, D.A., 2014. Emerging concepts in dendrimer-based nanomedicine: from design principles to clinical applications. J. Intern. Med. 276, 579–617. https://doi.org/10.1111/JOIM.12280

Kerr, J.F.R., Wyllie, A.H., Currie, A.R., 1972. Apoptosis: a basic biological phenomenon with wide-ranging implications in tissue kinetics. Br. J. Cancer 26, 239–257. https://doi.org/10.1038/BJC.1972.33

Kik, K., Bukowska, B., Sicińska, P., 2020. Polystyrene nanoparticles: Sources, occurrence in the environment, distribution in tissues, accumulation and toxicity to various organisms.

630 Environ. Pollut. 262. https://doi.org/10.1016/j.envpol.2020.114297

631 Kim, E.H., Choi, S., Kim, D., Park, H.J., Bian, Y., Choi, S.H., Chung, H.Y., Bae, O.N., 2022. Amine-
632 modified nanoplastics promote the procoagulant activation of isolated human red blood
633 cells and thrombus formation in rats. Part. Fibre Toxicol. 2022 191 19, 1–15.
634 https://doi.org/10.1186/S12989-022-00500-Y

635 Kwon, B.G., Saido, K., Koizumi, K., Sato, H., Ogawa, N., Chung, S.Y., Kusui, T., Kodera, Y.,
636 Kogure, K., 2014. Regional distribution of styrene analogues generated from polystyrene
637 degradation along the coastlines of the North-East Pacific Ocean and Hawaii. Environ.
638 Pollut. 188, 45–49. https://doi.org/10.1016/J.ENVPOL.2014.01.019

639 Leslie, H.A., van Velzen, M.J.M., Brandsma, S.H., Vethaak, A.D., Garcia-Vallejo, J.J., Lamoree,
640 M.H., 2022. Discovery and quantification of plastic particle pollution in human blood.
641 Environ. Int. 163, 107199. https://doi.org/10.1016/J.ENVINT.2022.107199

642 Liang, B., Zhong, Y., Huang, Y., Lin, X., Liu, J., Lin, L., Hu, M., Jiang, J., Dai, M., Wang, B., Zhang,
643 B., Meng, H., Lelaka, J.J.J., Sui, H., Yang, X., Huang, Z., 2021. Underestimated health risks:
644 polystyrene micro- and nanoplastics jointly induce intestinal barrier dysfunction by ROS-
645 mediated epithelial cell apoptosis. Part. Fibre Toxicol. 18.
646 https://doi.org/10.1186/S12989-021-00414-1

647 Liang, S., Yin, N., Faiola, F., 2019. Human Pluripotent Stem Cells as Tools for Predicting
648 Developmental Neural Toxicity of Chemicals: Strategies, Applications, and Challenges.
649 Stem Cells Dev. 28, 755–768. https://doi.org/10.1089/scd.2019.0007

650 Lins, T.F., O'Brien, A.M., Zargartalebi, M., Sinton, D., 2022. Nanoplastic State and Fate in
651 Aquatic Environments: Multiscale Modeling. Environ. Sci. Technol. 56, 4017–4028.
652 https://doi.org/10.1021/ACS.EST.1C03922/ASSET/IMAGES/LARGE/ES1C03922_0006.JPEG

653 Liste, I., García-García, E., Bueno, C., Martínez-Serrano, A., 2007. Bcl-XL modulates the
654 differentiation of immortalized human neural stem cells. Cell Death Differ. 14, 1880–
655 1892. https://doi.org/10.1038/sj.cdd.4402205

656 Liste, I., García-García, E., Martínez-Serrano, A., 2004. The Generation of Dopaminergic
657 Neurons by Human Neural Stem Cells Is Enhanced by Bcl-XL, Both In Vitro and In Vivo. J.
658 Neurosci. 24, 10786–10795. https://doi.org/10.1523/JNEUROSCI.3208-04.2004

659 Liu, A., Richards, L., Bladen, C.L., Ingham, E., Fisher, J., Tipper, J.L., 2015. The biological
660 response to nanometre-sized polymer particles. Acta Biomater. 23, 38–51.
661 https://doi.org/10.1016/J.ACTBIO.2015.05.016

662 Liu, L., Xu, K., Zhang, B., Ye, Y., Zhang, Q., Jiang, W., 2021. Cellular internalization and release of
663 polystyrene microplastics and nanoplastics. Sci. Total Environ. 779, 146523.
664 https://doi.org/10.1016/J.SCITOTENV.2021.146523

665 Liu, S., Lin, G., Liu, X., Yang, R., Wang, H., Sun, Y., Chen, B., Dong, R., 2023. Detection of various
666 microplastics in placentas, meconium, infant feces, breastmilk and infant formula: A pilot
667 prospective study. Sci. Total Environ. 854, 158699.
668 https://doi.org/10.1016/j.scitotenv.2022.158699

669 Liu, Y.Y., Liu, J., Wu, H., Zhang, Q., Tang, X.R., Li, D., Li, C.S., Liu, Y., Cao, A., Wang, H., 2022.
670 Endocytosis, Distribution, and Exocytosis of Polystyrene Nanoparticles in Human Lung
671 Cells. Nanomater. (Basel, Switzerland) 13. https://doi.org/10.3390/NANO13010084

672 Malinowska, K., Bukowska, B., Piwoński, I., Foksiński, M., Kisielewska, A., Zarakowska, E.,
673 Gackowski, D., Sicińska, P., 2022. Polystyrene nanoparticles: the mechanism of their
674 genotoxicity in human peripheral blood mononuclear cells. Nanotoxicology 16, 791–811.
675 https://doi.org/10.1080/17435390.2022.2149360

676 Malinowska, K., Sicińska, P., Michałowicz, J., Bukowska, B., 2023. The effects of non-
677 functionalized polystyrene nanoparticles of different diameters on the induction of
678 apoptosis and mTOR level in human peripheral blood mononuclear cells. Chemosphere
679 335. https://doi.org/10.1016/j.chemosphere.2023.139137

680 Mammo, F.K., Amoah, I.D., Gani, K.M., Pillay, L., Ratha, S.K., Bux, F., Kumari, S., 2020.
681 Microplastics in the environment: Interactions with microbes and chemical contaminants.
682 Sci. Total Environ. 743, 140518. https://doi.org/10.1016/j.scitotenv.2020.140518

683 Masud, R.I., Suman, K.H., Tasnim, S., Begum, M.S., Sikder, M.H., Uddin, M.J., Haque, M.N.,
684 2023. A review on enhanced microplastics derived from biomedical waste during the
685 COVID-19 pandemic with its toxicity, health risks, and biomarkers. Environ. Res. 216,
686 114434. https://doi.org/10.1016/J.ENVRES.2022.114434

687 Maul, J., Frushour, B.G., Kontoff, J.R., Eichenauer, H., Ott, K.-H., Schade, C., 2007. Polystyrene
688 and Styrene Copolymers. Ullmann's Encycl. Ind. Chem.
689 https://doi.org/10.1002/14356007.A21_615.PUB2

690 McMahon, H.T., Boucrot, E., 2011. Molecular mechanism and physiological functions of
691 clathrin-mediated endocytosis. Nat. Rev. Mol. Cell Biol. 12, 517–533.
692 https://doi.org/10.1038/NRM3151

693 McNeil, S.E., 2011. Challenges for Nanoparticle Characterization, Methods in Molecular

694 Biology. https://doi.org/10.1007/978-1-60327-198-1_2

695 Meyer, K., Kaspar, B.K., 2017. Glia-neuron interactions in neurological diseases: Testing non-
696 cell autonomy in a dish. Brain Res. 1656, 27–39.
697 https://doi.org/10.1016/J.BRAINRES.2015.12.051

698 Olney, J.W., 2014. Focus on apoptosis to decipher how alcohol and many other drugs disrupt
699 brain development. Front. Pediatr. 2. https://doi.org/10.3389/FPED.2014.00081

700 Peng, L., Fu, D., Qi, H., Lan, C.Q., Yu, H., Ge, C., 2020. Micro- and nano-plastics in marine
701 environment: Source, distribution and threats — A review. Sci. Total Environ. 698,
702 134254. https://doi.org/10.1016/J.SCITOTENV.2019.134254

703 Pitt, J.A., Trevisan, R., Massarsky, A., Kozal, J.S., Levin, E.D., Di Giulio, R.T., 2018. Maternal
704 transfer of nanoplastics to offspring in zebrafish (Danio rerio): A case study with
705 nanopolystyrene. Sci. Total Environ. 643, 324–334.
706 https://doi.org/10.1016/J.SCITOTENV.2018.06.186

707 Plastic Pollution Facts | PlasticOceans.org/the-facts [WWW Document], n.d. URL
708 https://plasticoceans.org/the-facts/ (accessed 10.31.23).

709 Plastics Europe • Enabling a sustainable future [WWW Document], n.d. URL
710 https://plasticseurope.org/ (accessed 3.9.23).

711 Plastics the fast facts 2023 : A review on plastic contributions to European economy, 2023. .
712 2023 2023.

713 Popova, N. V., Deyev, I.E., Petrenko, A.G., 2013. Clathrin-mediated endocytosis and adaptor
714 proteins. Acta Naturae 5, 62–73. https://doi.org/10.32607/20758251-2013-5-3-62-73

715 Rafiee, M., Dargahi, L., Eslami, A., Beirami, E., Jahangiri-rad, M., Sabour, S., Amereh, F., 2018.
716 Neurobehavioral assessment of rats exposed to pristine polystyrene nanoplastics upon
717 oral exposure. Chemosphere 193, 745–753.
718 https://doi.org/10.1016/J.CHEMOSPHERE.2017.11.076

719 Ragusa, A., Svelato, A., Santacroce, C., Catalano, P., Notarstefano, V., Carnevali, O., Papa, F.,
720 Rongioletti, M.C.A., Baiocco, F., Draghi, S., D'Amore, E., Rinaldo, D., Matta, M., Giorgini,
721 E., 2021. Plasticenta: First evidence of microplastics in human placenta. Environ. Int. 146,
722 106274. https://doi.org/10.1016/J.ENVINT.2020.106274

723 Rahman, M.M., Islam, M.R., Yamin, M., Islam, M.M., Sarker, M.T., Meem, A.F.K., Akter, A.,
724 Emran, T. Bin, Cavalu, S., Sharma, R., 2022. Emerging Role of Neuron-Glia in Neurological

725 Disorders: At a Glance. Oxid. Med. Cell. Longev. 2022.
726 https://doi.org/10.1155/2022/3201644

727 Rosca, A., Coronel, R., López-Alonso, V., Liste, I., González-Caballero, M.C., 2023. Human neural
728 stem cells in developmental neurotoxicology: Current scenario and future prospects.
729 Academic Press. https://doi.org/10.1016/bs.ant.2023.01.005

730 Rosca, A., Coronel, R., Moreno, M., González, R., Oniga, A., Martín, A., López, V., González, M.
731 del C., Liste, I., 2020. Impact of environmental neurotoxic: current methods and
732 usefulness of human stem cells. undefined 6.
733 https://doi.org/10.1016/J.HELIYON.2020.E05773

734 Sachse, M., Urbé, S., Oorschot, V., Strous, G.J., Klumperman, J., 2002. Bilayered clathrin coats
735 on endosomal vacuoles are involved in protein sorting toward lysosomes. Mol. Biol. Cell
736 13, 1313–1328. https://doi.org/10.1091/MBC.01-10-0525

737 Sandoval, L., Rosca, A., Oniga, A., Zambrano, A., Ramos, J.J., González, M.C., Liste, I., Motas, M.,
738 2019. Effects of chlorpyrifos on cell death and cellular phenotypic specification of human
739 neural stem cells. Sci. Total Environ. 683, 445–454.
740 https://doi.org/10.1016/J.SCITOTENV.2019.05.270

741 Sarma, D.K., Dubey, R., Samarth, R.M., Shubham, S., Chowdhury, P., Kumawat, M., Verma, V.,
742 Tiwari, R.R., Kumar, M., 2022. The Biological Effects of Polystyrene Nanoplastics on
743 Human Peripheral Blood Lymphocytes. Nanomater. (Basel, Switzerland) 12.
744 https://doi.org/10.3390/NANO12101632

745 Schwabl, P., Koppel, S., Konigshofer, P., Bucsics, T., Trauner, M., Reiberger, T., Liebmann, B.,
746 2019. Detection of various microplastics in human stool: A prospective case series. Ann.
747 Intern. Med. 171, 453–457. https://doi.org/10.7326/M19-0618/SUPPL_FILE/M19-
748 0618_SUPPLEMENT.PDF

749 Shan, S., Zhang, Y., Zhao, H., Zeng, T., Zhao, X., 2022. Polystyrene nanoplastics penetrate across
750 the blood-brain barrier and induce activation of microglia in the brain of mice.
751 Chemosphere 298, 134261. https://doi.org/10.1016/J.CHEMOSPHERE.2022.134261

752 Shi, X., Wang, X., Huang, R., Tang, C., Hu, C., Ning, P., Wang, F., 2022. Cytotoxicity and
753 Genotoxicity of Polystyrene Micro- and Nanoplastics with Different Size and Surface
754 Modification in A549 Cells. Int. J. Nanomedicine 17, 4509–4523.
755 https://doi.org/10.2147/IJN.S381776

756 Song, K., Ding, R., Sun, C., Yao, L., Zhang, W., 2021. Microparticles and microplastics released

from daily use of plastic feeding and water bottles and plastic injectors: potential risks to infants and children in China. Environ. Sci. Pollut. Res. 28, 59813–59820. https://doi.org/10.1007/S11356-021-14939-7/FIGURES/3

Song, Y., Li, X., Du, X., 2009. Exposure to nanoparticles is related to pleural effusion, pulmonary fibrosis and granuloma. Eur. Respir. J. 34, 559–567. https://doi.org/10.1183/09031936.00178308

Stapleton, P.A., 2019. Toxicological considerations of nano-sized plastics. AIMS Environ. Sci. 6, 367–378. https://doi.org/10.3934/ENVIRONSCI.2019.5.367

Tanvig, M., Blaabjerg, M., Andersen, R.K., Villa, A., Rosager, A.M., Poulsen, F.R., Martinez-Serrano, A., Zimmer, J., Meyer, M., 2009. A brain slice culture model for studies of endogenous and exogenous precursor cell migration in the rostral migratory stream. Brain Res. 1295, 1–12. https://doi.org/10.1016/j.brainres.2009.07.075

Torres-ruiz, M., Alba, M. De, Morales, M., Martin-folgar, R., Carmen, M., Cañas-portilla, A.I., De, A., 2023. Science of the Total Environment Neurotoxicity and endocrine disruption caused by polystyrene nanoparticles in zebra fi sh embryo. Sci. Total Environ. 874, 162406. https://doi.org/10.1016/j.scitotenv.2023.162406

Torres-Ruiz, M., De la Vieja, A., de Alba Gonzalez, M., Esteban Lopez, M., Castaño Calvo, A., Cañas Portilla, A.I., 2021. Toxicity of nanoplastics for zebrafish embryos, what we know and where to go next. Sci. Total Environ. 797. https://doi.org/10.1016/J.SCITOTENV.2021.149125

Villa, A., Snyder, E.Y., Vescovi, A., Martínez-Serrano, A., 2000. Establishment and properties of a growth factor-dependent, perpetual neural stem cell line from the human CNS. Exp. Neurol. 161, 67–84. https://doi.org/10.1006/EXNR.1999.7237

Walczak, A.P., Kramer, E., Hendriksen, P.J.M., Tromp, P., Helsper, J.P.F.G., Van Der Zande, M., Rietjens, I.M.C.M., Bouwmeester, H., 2015. Translocation of differently sized and charged polystyrene nanoparticles in in vitro intestinal cell models of increasing complexity. http://dx.doi.org/10.3109/17435390.2014.944599 9, 453–461. https://doi.org/10.3109/17435390.2014.944599

Wang, T., Wang, Lu, Li, X., Hu, X., Han, Y., Luo, Y., Wang, Z., Li, Q., Aldalbahi, A., Wang, Lihua, Song, S., Fan, C., Zhao, Y., Wang, M., Chen, N., 2017. Size-Dependent Regulation of Intracellular Trafficking of Polystyrene Nanoparticle-Based Drug-Delivery Systems. ACS Appl. Mater. Interfaces 9, 18619–18625. https://doi.org/10.1021/ACSAMI.7B05383

789 Weber, A., Schwiebs, A., Solhaug, H., Stenvik, J., Nilsen, A.M., Wagner, M., Relja, B., Radeke,
790 H.H., 2022. Nanoplastics affect the inflammatory cytokine release by primary human
791 monocytes and dendritic cells. Environ. Int. 163.
792 https://doi.org/10.1016/J.ENVINT.2022.107173

793 Wu, J., Jiang, R., Lin, W., Ouyang, G., 2019. Effect of salinity and humic acid on the aggregation
794 and toxicity of polystyrene nanoplastics with different functional groups and charges.
795 Environ. Pollut. 245, 836–843. https://doi.org/10.1016/j.envpol.2018.11.055

796 Xie, H., Tian, X., Lin, X., Chen, R., Hameed, S., Wang, L., Yu, Y.L., Li, B., Li, Y.F., 2023.
797 Nanoplastic-Induced Biological Effects In Vivo and In Vitro: An Overview. Rev. Environ.
798 Contam. Toxicol. 261. https://doi.org/10.1007/s44169-023-00027-z

799 Yang, M., Wang, W.X., 2023. Recognition and movement of polystyrene nanoplastics in fish
800 cells. Environ. Pollut. 316, 120627. https://doi.org/10.1016/j.envpol.2022.120627

801 Yuan, J., Ma, J., Sun, Y., Zhou, T., Zhao, Y., Yu, F., 2020. Microbial degradation and other
802 environmental aspects of microplastics/plastics. Sci. Total Environ. 715, 136968.
803 https://doi.org/10.1016/j.scitotenv.2020.136968

804 Zalasiewicz, J., Waters, C.N., Ivar do Sul, J.A., Corcoran, P.L., Barnosky, A.D., Cearreta, A.,
805 Edgeworth, M., Gałuszka, A., Jeandel, C., Leinfelder, R., McNeill, J.R., Steffen, W.,
806 Summerhayes, C., Wagreich, M., Williams, M., Wolfe, A.P., Yonan, Y., 2016. The
807 geological cycle of plastics and their use as a stratigraphic indicator of the Anthropocene.
808 Anthropocene 13, 4–17. https://doi.org/10.1016/J.ANCENE.2016.01.002

809 Zhang, T., Yang, S., Ge, Y., Wan, X., Zhu, Y., Li, J., Yin, L., Pu, Y., Liang, G., 2022. Polystyrene
810 Nanoplastics Induce Lung Injury via Activating Oxidative Stress: Molecular Insights from
811 Bioinformatics Analysis. Nanomater. (Basel, Switzerland) 12.
812 https://doi.org/10.3390/NANO12193507

813

A

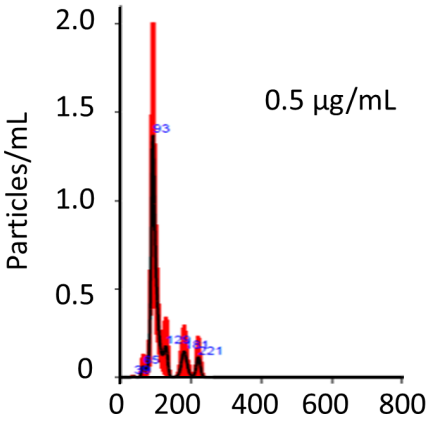

B

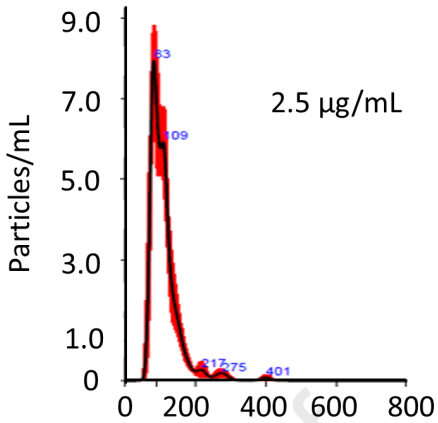

C

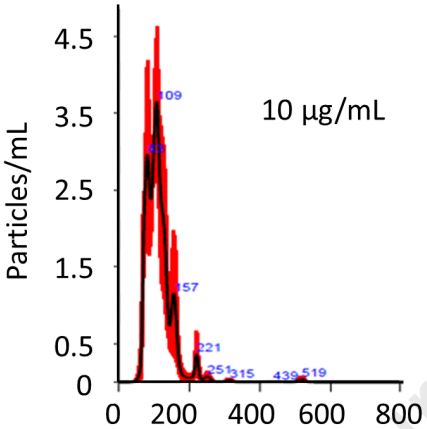

D

NP (ug/L)	Aggregate Size (nm)	Zeta Potential (mV)
0.5	112.4±37.5	-25.4±1.06
2.5	112.0±44.2	-33.8±1.30
10	115.5±43.9	-33.95±0.64

E

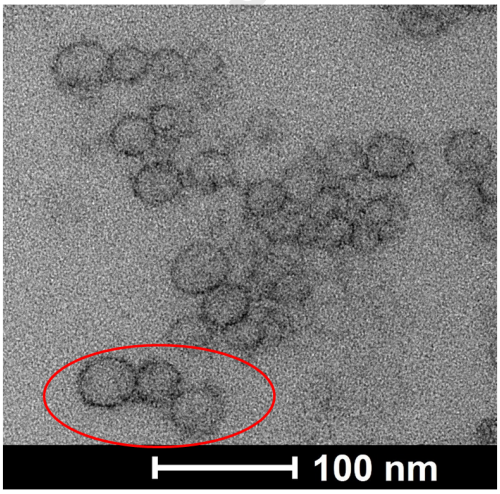

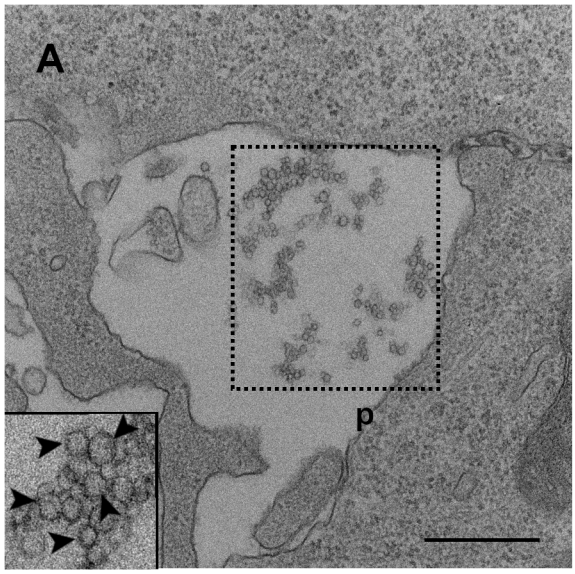
A
p

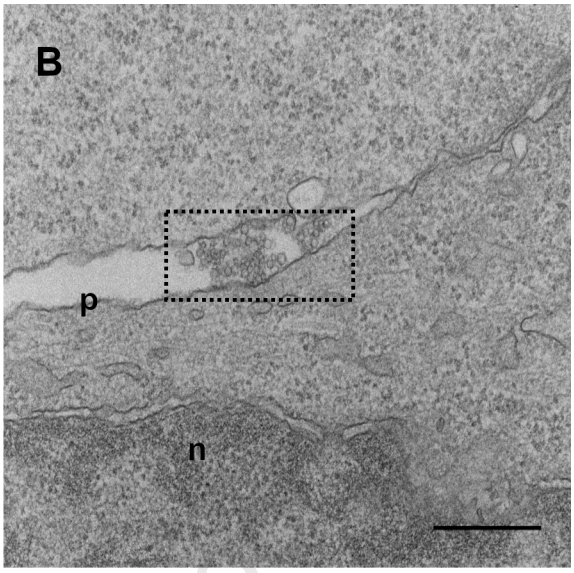
B
p
n

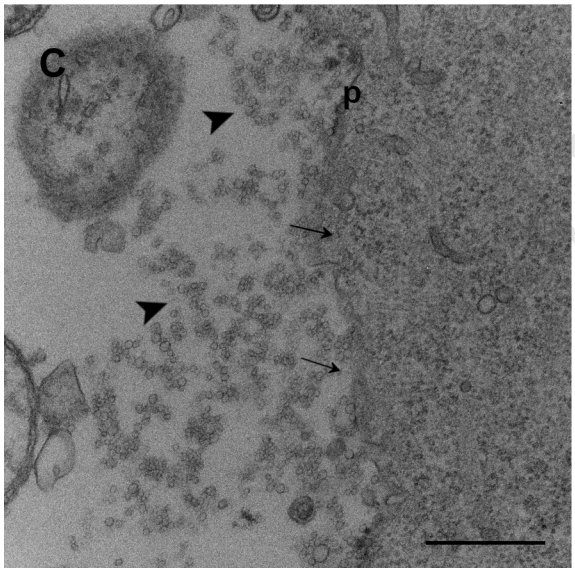
C
p

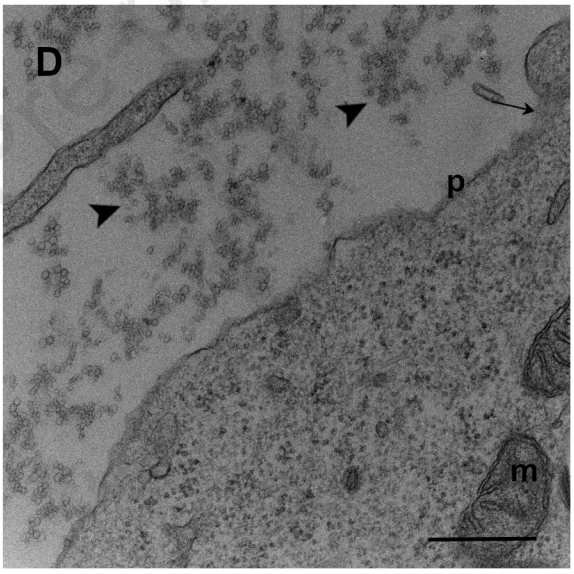
D
p
m

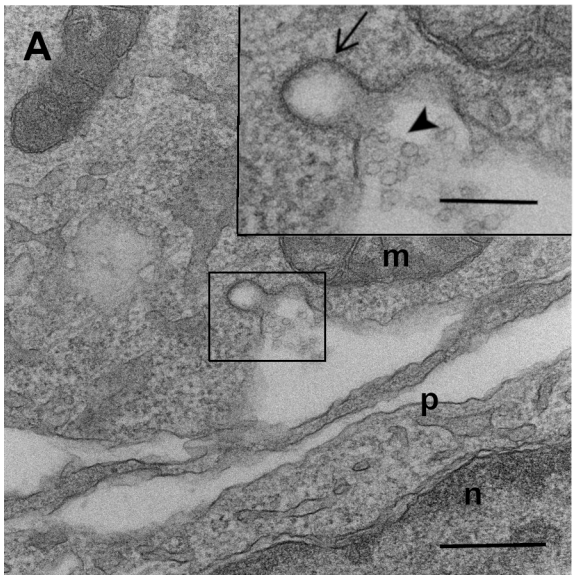

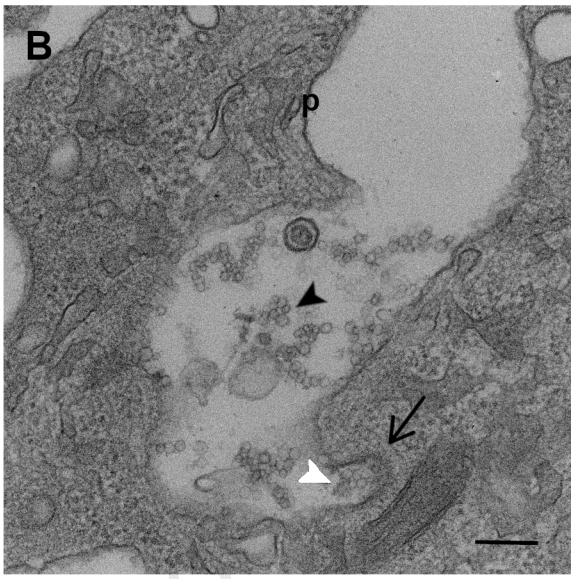

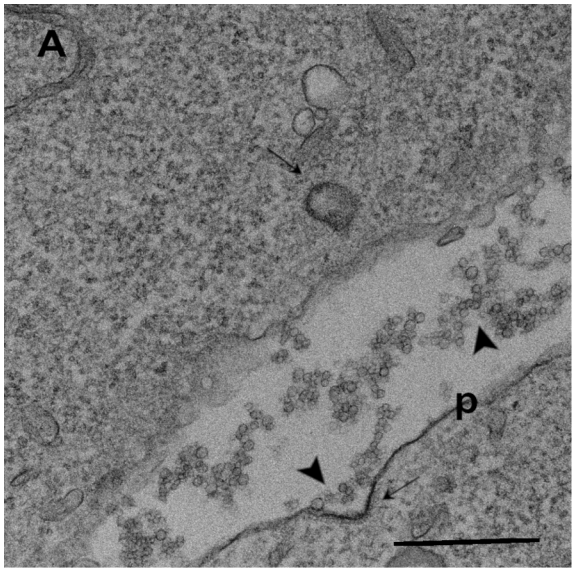

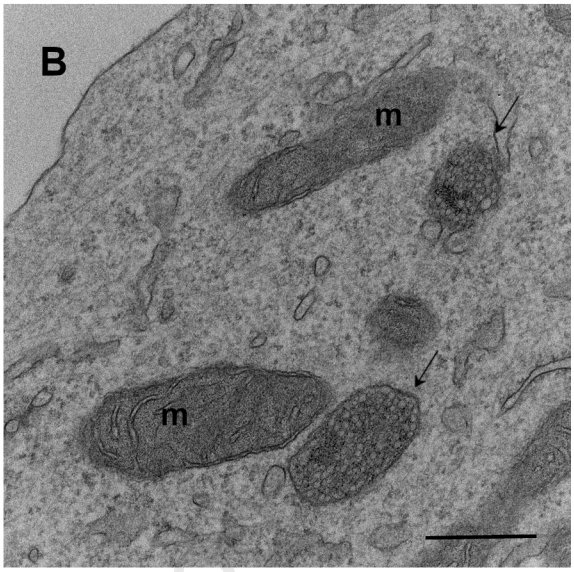

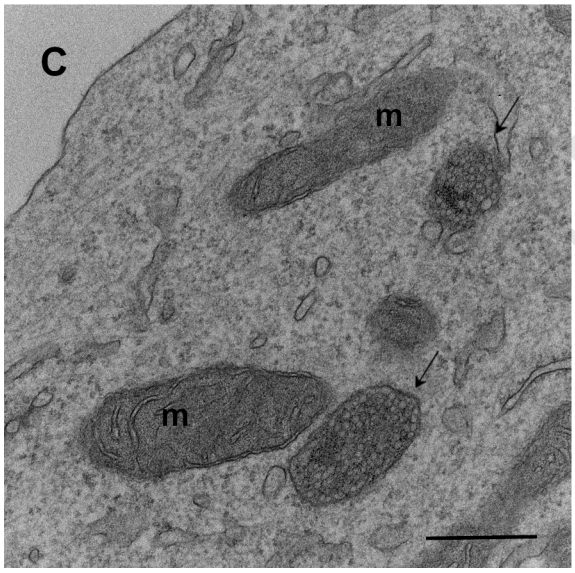

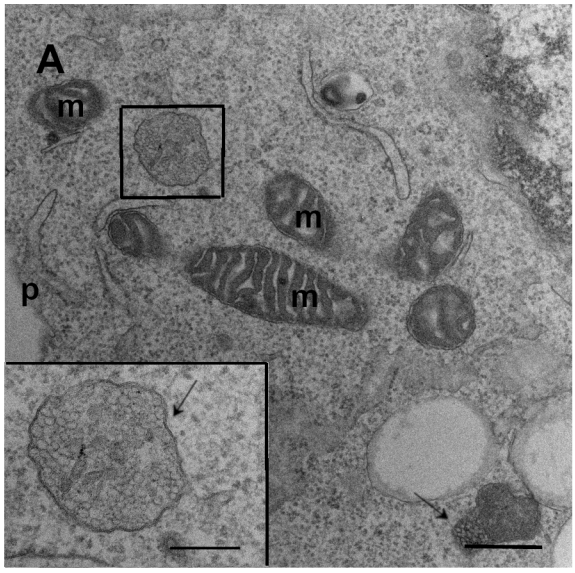
A
m
m
m
p

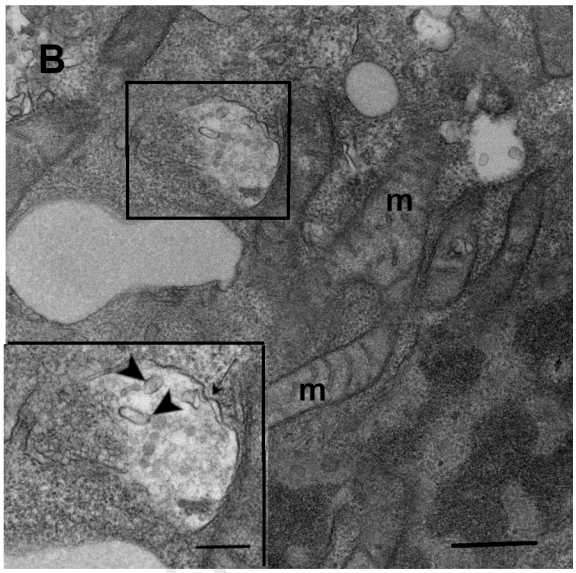
B
m
m

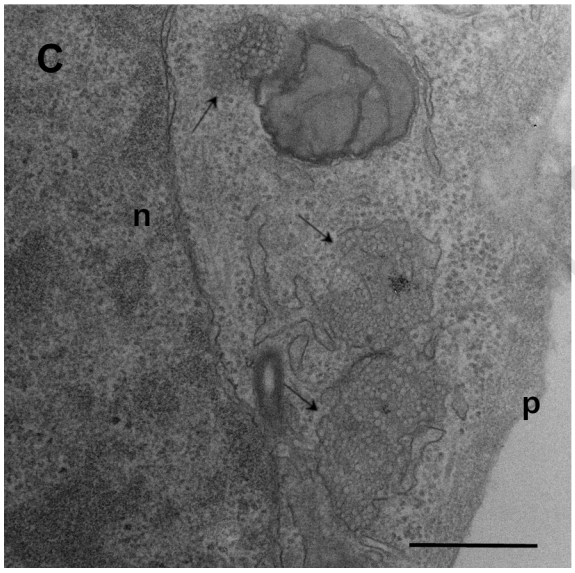
C
n
p

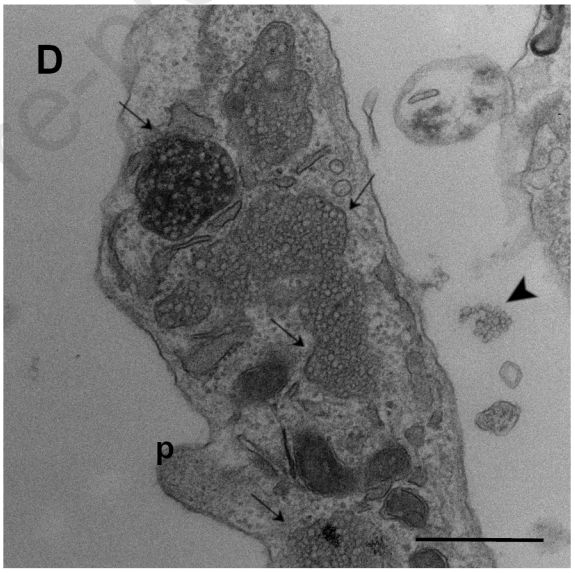
D
p

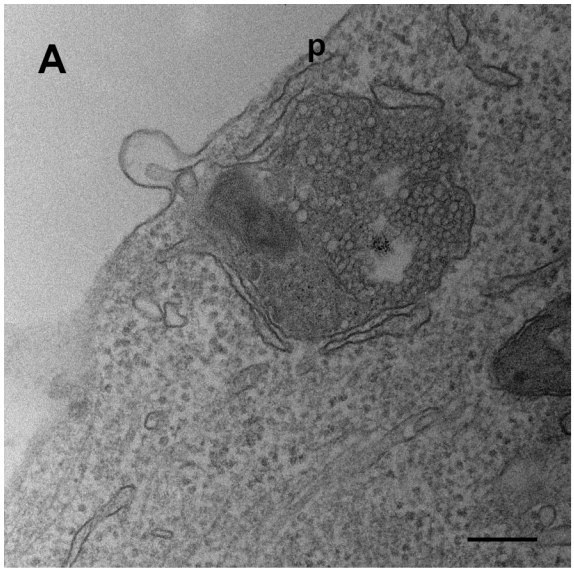

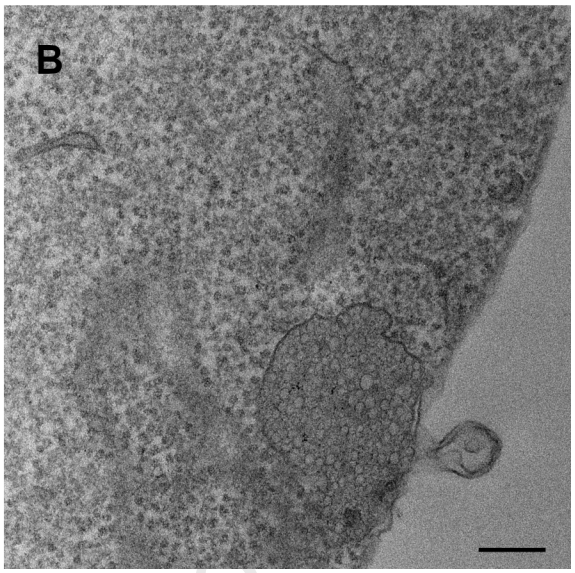

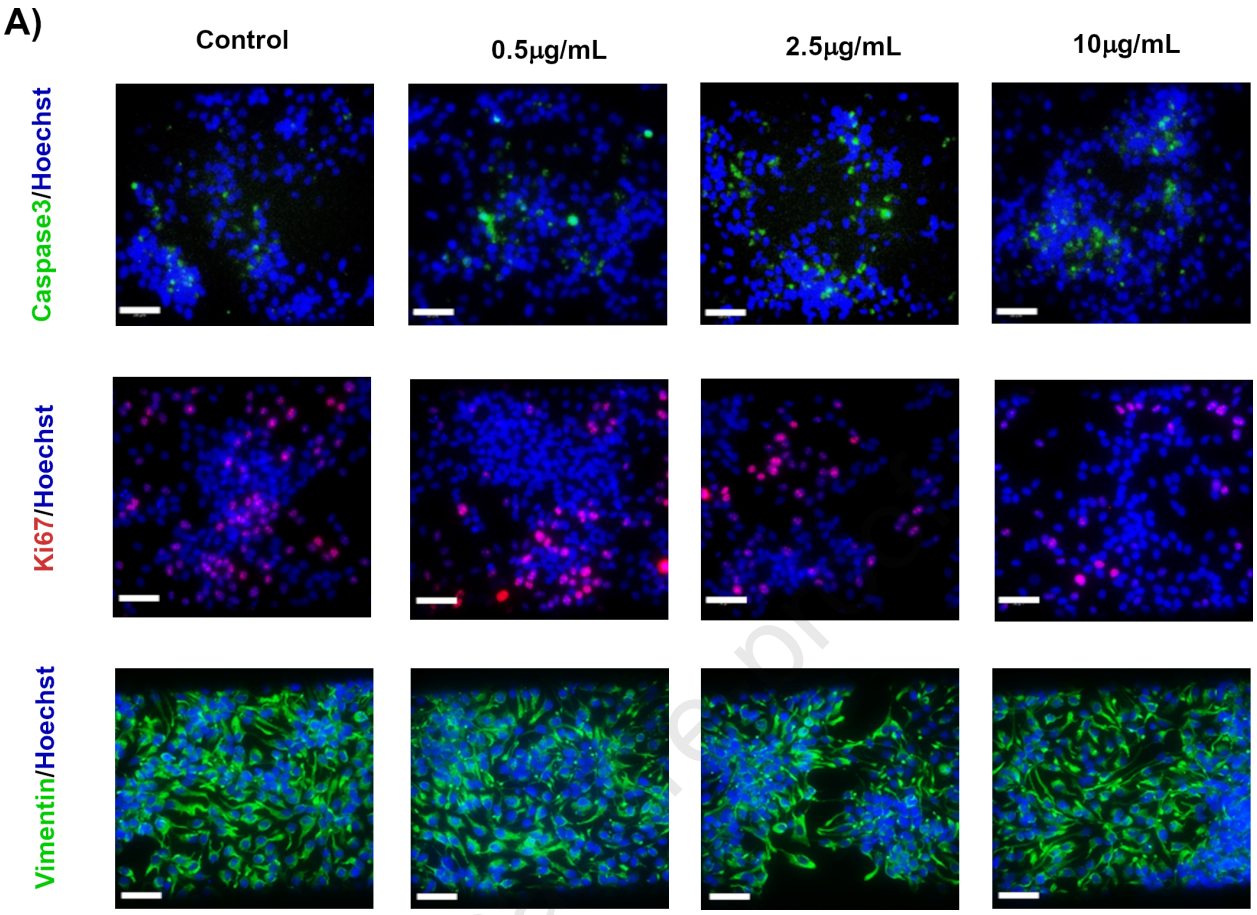
A)
Control
0.5µg/mL
2.5µg/mL
10µg/mL
Caspase3/Hoechst
Ki67/Hoechst
Vimentin/Hoechst

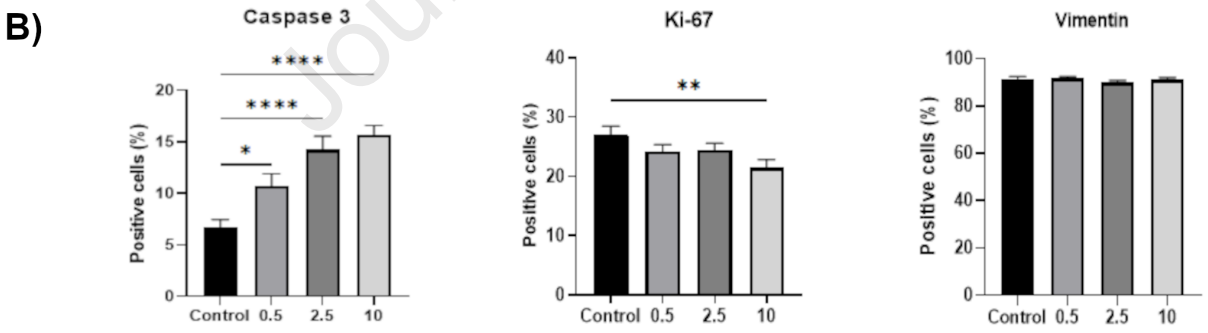
B)
Caspase 3
Positive cells (%)
Control 0.5 2.5 10
Ki-67
Positive cells (%)
Control 0.5 2.5 10
Vimentin
Positive cells (%)
Control 0.5 2.5 10

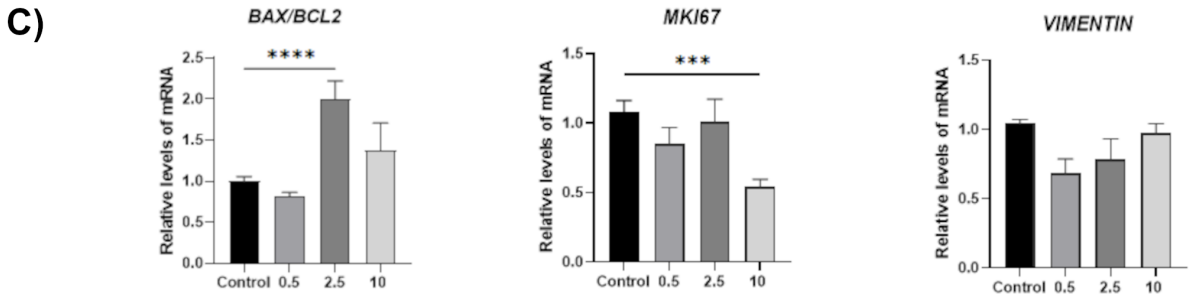
C)
BAX/BCL2
Relative levels of mRNA
Control 0.5 2.5 10
MKI67
Relative levels of mRNA
Control 0.5 2.5 10
VIMENTIN
Relative levels of mRNA
Control 0.5 2.5 10

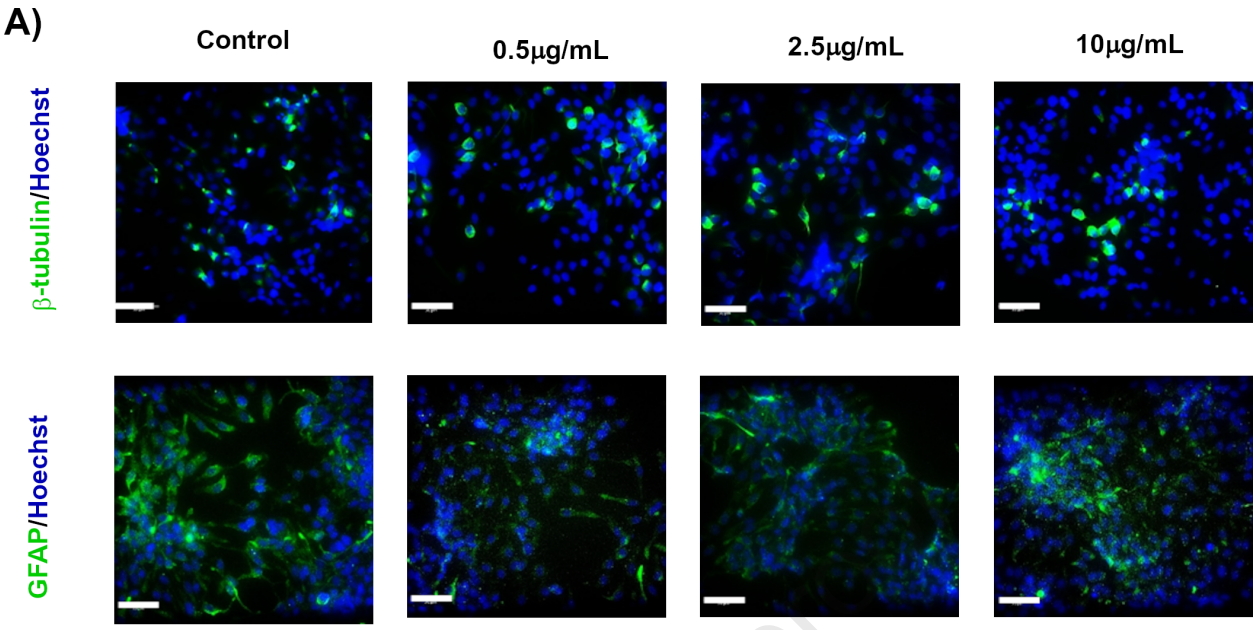

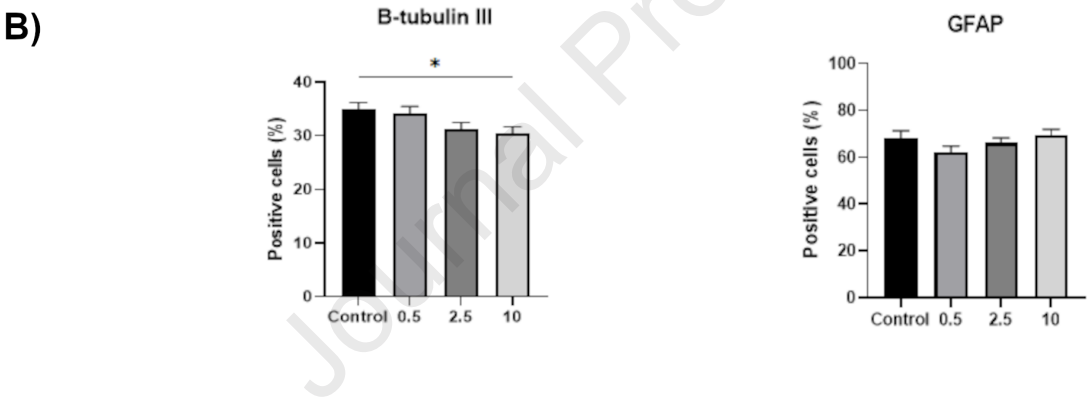

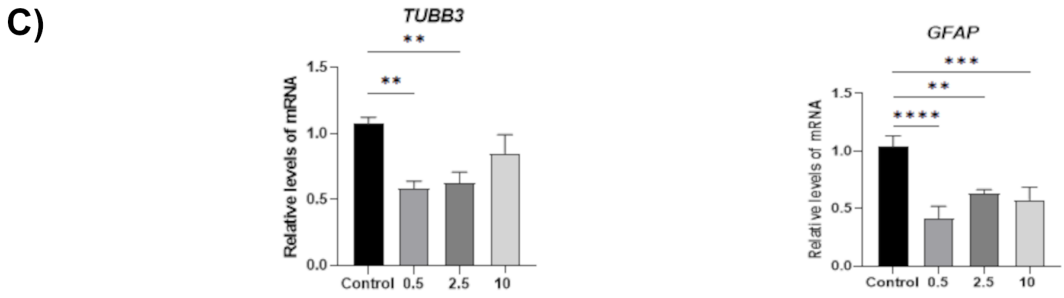

Highlights

- 30 nm PS-NPs enter the human NSC by endocytosis without being detected in the nucleus
- PS-NPs were localized and aggregated in endosomes and vacuoles of hNS1 cells
- PS-NPs caused cell death by apoptosis and decreased cell proliferation

Declaration of interests

☒ The authors declare that they have no known competing financial interests or personal relationships that could have appeared to influence the work reported in this paper.

☐ The authors declare the following financial interests/personal relationships which may be considered as potential competing interests: